CONTRACT SERIAL NO. 23440-0-9036-01-SS
CONTRACTOR: Univ. N.B.

THE DEVELOPMENT OF A FLOWMETER FOR MEASURING ASH RECIRCULATION RATES IN FLUIDIZED BED COMBUSTORS

By

M. F. Couturier
Energy Conversion Engineering Group
University of New Brunswick
Fredericton, NB, Canada
E3B 5A3

A report to

Energy, Mines and Resources Canada
Energy Research Laboratories, CANMET
Ottawa, Canada

March 1991

PREFACE

This is the final report on work performed under a contract with Supply and Services Canada:

SSC Contract Serial No.: 23440-0-9036/01-SS

SSC File No.: 055SS.23440-0-9036

Title: The Development of a Flowmeter for Measuring Ash Recirculation Rates in Fluidized Bed Combustors

Principal Investigator: Dr. Michel F. Couturier, Associate Professor
Chemical Engineering Department
University of New Brunswick
Fredericton, NB, Canada, E3B 5A3
Telephone: (506) 453-4520

Scientific Authority: Mr. V. Razbin, Dept. of Energy, Mines and Resources
CANMET-MLS Division
555 Booth Street
Ottawa, Ontario, K1A 0G1
Telephone: (613) 996-4567

Science Branch Contracting Officer: Mr. P.J. Monelly, Science and Professional Services Directorate, Supply and Services Canada, 12C1 Place du Portage - Phase III
11 Laurier Street
Hull, Quebec, K1A 0S5
Telephone: (819) 956-1683

Commencement Date: 07 June, 1990

Delivery Date: 29 March, 1991

ACKNOWLEDGEMENTS

I am grateful to Messrs. Tom Chapman and Todd Pugsley for their help in taking the heat transfer measurements within the downcomer of the CFB unit at UNB and to Mr. Viken Najarian for his assistance during the on-site testing of the ash flowmeter. The cooperation received from Mr. Emmete Kelly and his staff of the fluidized bed boiler plant at CFB Summerside is also gratefully acknowledged. Their support and helpful comments have greatly facilitated our on-site work. Finally I would like to thank Mr. Orville Scott for his photographic contribution to the project and express my sincere gratitude to Messrs. Alfred Knappe and Brian Hawkins for their suggestions and meticulous work during the construction of the heat exchanger and heat flux probe.

CONTENTS

PAGE

1. Introduction

2. Review of Techniques for Measuring Ash Recirculation Rates

3. Flowmeter for Measuring the Ash Recirculation Rate in the No. 2 FBC Boiler at CFB Summerside

4. Project Schedule

5. Heat Transfer Measurements in the Return Leg of the UNB Circulating Fluidized Bed

6. Results and Discussion

   6.1 Heat Transfer between a Horizontal Cylinder and a Moving Packed Bed of Sand

   6.2 Performance of the Ash Flowmeter

7. Conclusion

8. Recommendations

9. References

FIGURES

PAGE

1. Heat Exchanger for Measuring Solids Recirculation Rate
2. Heat Exchangers Previously Used to Measure Ash Recirculation Rates in Pilot-Scale FBC Units
3. The Ash Recirculation Loop at CFB Summerside
4. Heat Exchanger for Measuring Ash Recirculation Rate at CFB Summerside
5. Cooling Water Distribution Within the Heat Exchanger
6. Radial Location of Ash Thermocouples
7. Side View of the Heat Exchanger
8. End View of the Heat Exchanger
9. Inside View of the Heat Exchanger
10. Cold Circulating Fluidized Bed Model at UNB
11. Schematic of the Cylindrical Heat Transfer Probe
12. Copper Sleeve Equipped with Circular Fins
13. Average Heat Transfer Coefficient Over Horizontal Cylinders Immersed in a Downward Moving Packed Bed of Sand
14. Downward Flow of Solid Particles over a Horizontal Cylinder
15. Solids Flux in the Downcomer versus Particle Velocity next to the Wall
16. Particle Size Distributions of the Cyclone Ash from CFB Summerside and Sand in the Circulating Fluidized Bed at UNB
17. Possible Ash Flow Patterns in Return Pipe
18. Temperature Distribution of the Ash at the Heat Exchanger Inlet

TABLES

PAGE

1. Ash Flow Measuring Techniques

2. Design Specifications for Ash Flowmeter

3. Properties of Sand Material

4. Chemical Composition of the Cyclone Ash from CFB Summerside

5. Heat Capacity of Cyclone Ash

6. Results of Tests Performed on Ash Flowmeter

7. Overall Heat Transfer Coefficient over each Bayonet Bundle

NOTATION

Variables:

$\bar{a}$	variable defined in Eq. (4), dimensionless
A	surface area exposed to the solids, m^2
Cp	heat capacity, J/g K
D	diameter of bayonet or heat transfer probe, m
F	solids flux, g/s
h	average heat transfer coefficient, W/m^2 K
I	current, A
k	thermal conductivity, W/m K
l	length of stainless steel ring, m
L	length of middle heater, m
m	mass flowrate, g/s
r	radial position, m
R	inside radius of return pipe, m
t	thickness of stainless steel ring, m
T	temperature, K
u	particle velocity, m
U	overall heat transfer coefficient, W/m^2 K
V	voltage, v
x	mass fraction
η	fin efficiency
θ	angle
ρ	bulk density of solids, g/m^3

Subscripts:

avg	mean
b	bayonet
cyl	cylinder
end	end heater
i	inside
middle	middle heater
o	outside
r	ring
s	solids
w	water
1	inlet
2	outlet

1. INTRODUCTION

The ash recirculation rate is a key variable in the operation of fluidized bed combustors (FBC). An increase in the ash recirculation rate usually has the beneficial effect of increasing heat transfer, sulphur capture and combustion efficiency but can also have the detrimental effect of increasing fan power and erosion within the combustor. The control of the ash recirculation rate in fluidized bed combustors is however difficult because operators must rely on crude techniques, such as measuring the pressure drop near the top of the combustor[1], to estimate the flowrate of the recirculated ash. There is thus a need to devise a flowmeter for on-line measurement of the ash recirculation rate in industrial bubbling and circulating fluidized beds.

The development of a flowmeter for measuring the ash recirculation rate in bubbling fluidized bed combustors is described in this report. The operating principle of the flowmeter is based on estimating the solids flow from a heat balance around a heat exchanger located in the ash return line. The proposed concept was tested by building a prototype for the No. 2 fluidized bed boiler at Canadian Forces Base Summerside in the province of Prince Edward Island. The objectives of this work were

- to demonstrate that the ash recirculation rate in commercial fluidized bed combustors can be reliably measured using the ash flowmeter design proposed herein and
- to measure the ash recirculation rate within the No. 2 FBC boiler at CFB Summerside.

The Summerside fluidized bed plant was ideal for testing the ash flowmeter. First of all, because the plant is an industrial facility, the concept was demonstrated in a commercial setting. Furthermore the plant is of medium scale so that the size and cost of the flowmeter were reasonable. Finally the design

of the ash recirculation loop at CFB Summerside is such that it was relatively easy to install and test the ash flowmeter. The recycled ash could be collected in barrels and weighed to verify the recirculation rate measured with the flowmeter.

2. REVIEW OF TECHNIQUES FOR MEASURING ASH RECIRCULATION RATES

An acceptable device for measuring the ash recirculation rate in fluidized bed combustors must

- be rugged with as few moving parts as possible,
- be capable of operating at high temperature and in large units,
- provide a continuous measurement without obstructing the ash flow, and
- require negligible attention from the operators once installed.

Of the seven experimental techniques presented in Table 1 and which have been used in the past to measure ash recirculation rates in bubbling or circulating fluidized beds, only the heat exchanger concept used by Burkell et al.[4] and Salib[5] meets the above requirements. In this concept, the ash flow is simply obtained by conducting a heat balance around a heat exchanger as shown in Fig. 1. If heat losses to the surroundings and the interstitial air are ignored, then the solids flowrate can be obtained using the following equation,

$$m_s = \frac{m_w * Cp_w * (T_{w,2} - T_{w,1})}{Cp_s * (T_{s,1} - T_{s,2})} \qquad (1)$$

where m is mass flowrate, T is bulk temperature, Cp is the heat capacity, the subscript w is for the cooling water and the subscript s is for the solids, and the subscripts 1 and 2 designate inlet and outlet conditions, respectively. The heat exchanger is normally installed prior to the J valve in the ash recirculation loop at a point where the ash moves in packed-bed mode.

The design of a heat exchanger for measuring solids recirculation rates in fluidized bed combustors must be such that

- the flow of the solids is not hampered by the heat exchanger, and
- the exit temperature of the solids is nearly uniform in the lateral direction.

Table 1. Ash Flow Measuring Techniques

	Operating Principle	Ref.
1.	Integration of the mass flux profile obtained with a solid sampling probe at the exit of the fluidized bed.	(1)
2.	Momentary diversion of the recycled ash stream into a collecting vessel.	(2)
3.	Measurement of the ash buildup rate on a permeable valve located in the return leg while it is momentarily closed.	(3,4)
4.	Timing of the descent of identifiable particles in the vertical standpipe of the return system.	(4)
5	Recording of the force imparted on a plate by returning solids.	(4)
6.	Measurement of the pressure drop across a constriction in the return loop.	(4)
-	Estimation of the solids flow from a heat balance on a calorimetric section in the return loop.	(4,5)

heat balance:

$$m_s = \frac{m_w * Cp_w * (T_{w2} - T_{w1})}{Cp_s * (T_{s1} - T_{s2})}$$

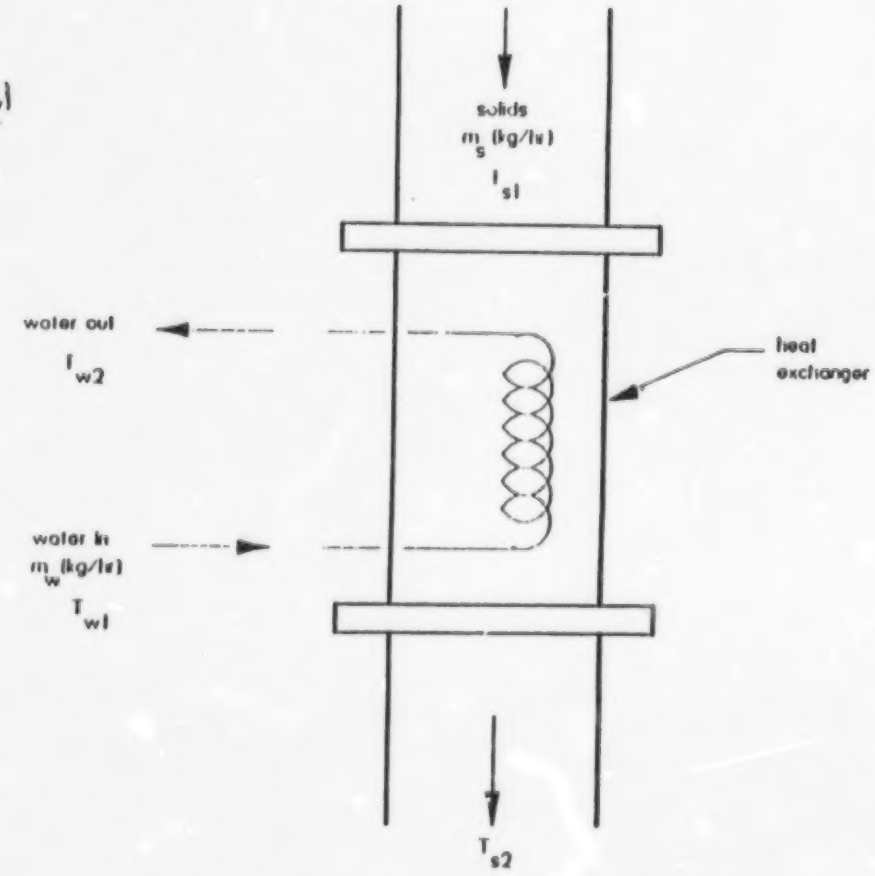

FIG. 1 HEAT EXCHANGER FOR MEASURING SOLIDS RECIRCULATION RATE

This last point is especially important because the velocity profile of the solids leaving the heat exchanger is normally unknown and as a result the estimate of the bulk exit temperature $T_{s,2}$ can be grossly in error when there is a significant temperature gradient at the outlet of the heat exchanger. For this reason, the double-pipe heat exchanger design shown in Fig. 2 is not suitable for large ash recirculating loops because the temperature of the leaving solids will be highly non-uniform.

The staggered-tube arrangement, also shown in Fig. 2, avoids the latter problem by providing a more uniform cooling of the solids stream. Also this design by providing a large surface area for heat transfer per unit volume leads to fairly compact heat exchangers. However because the tubes must be mounted on flat plates, the heat exchanger must necessarily be of rectangular shape and transition pieces must be mounted on its ends when it is installed in circular ash recirculation pipes. Furthermore the bulky design of the staggered-tube arrangement is not well suited for installation on ash recirculation pipes with little unobstructed space around them (like the ones on the FBC boilers at CFB Summerside).

The next section will outline the design of a heat exchanger that attempts to exploit the advantages of the staggered-tube and double-pipe arrangements.

3. FLOWMETER FOR MEASURING THE ASH RECIRCULATION RATE IN THE NO. 2 FBC BOILER AT CFB SUMMERSIDE

A schematic of the bottom section of the solids recirculation loop on the No. 2 FBC boiler at CFB Summerside is shown in Fig. 3. The solid particles leaving the fluidized bed are separated from the flue gas by a cyclone and then fall into a hopper before being divided into two streams which fall back into the combustor along a 6" schedule 80 pipe (0.146 m I.D. x 0.168 m O.D.) at 45°. Only one of the two ash return pipes on unit No. 2 is shown in Fig. 3. At the bottom

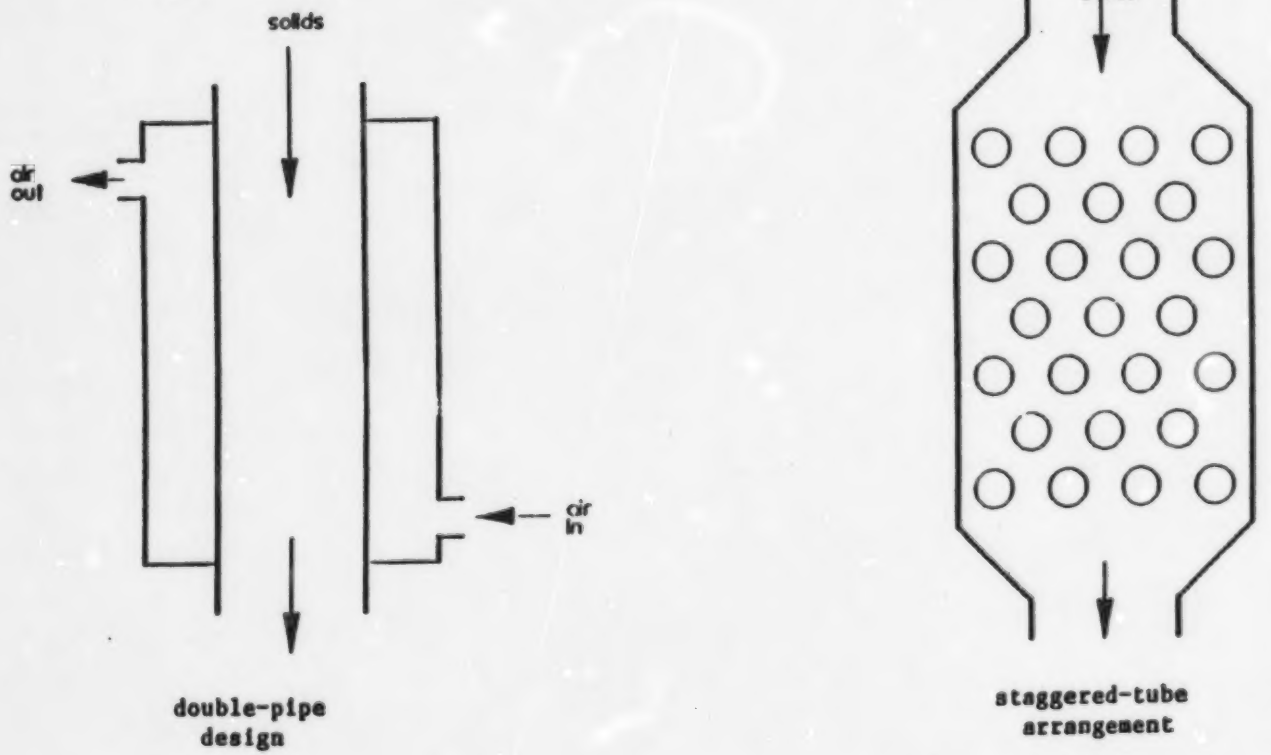

FIG. 2 HEAT EXCHANGERS PREVIOUSLY USED TO MEASURE ASH RECIRCULATION RATES IN PILOT-SCALE FBC UNITS

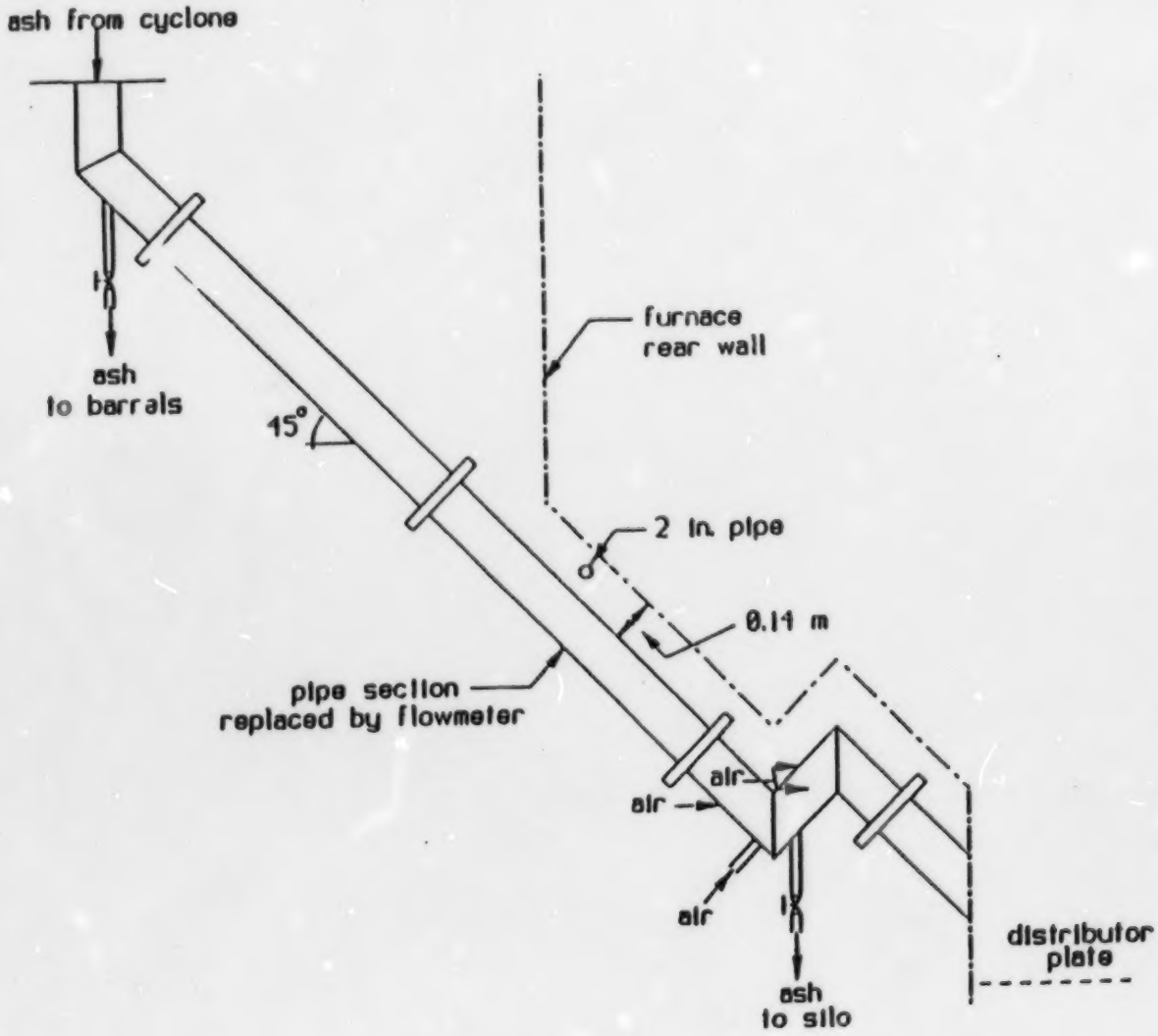

FIG. 3 THE ASH RECIRCULATION LOOP AT CFB SUMMERSIDE

of each return pipe there is a J valve on which four air lances are mounted to keep the solid particles moving. The ash particles enter the fluidized bed about 20 cm above the distributor plate. Two ash drain lines are located on each return pipe: One at the J valve and one below the cyclone hopper.

The ash flowmeter was installed in place of the 2.5 m long flanged pipe section above the J-valve as shown in Fig. 3. At that location the distance between the slopping furnace wall and the return pipe is 14 cm and at one point a horizontal 2" pipe, also shown in Fig. 3, is only 4 cm above the return pipe. Because of the limited head room, the overall diameter of the flowmeter could not be significantly larger than that of the pipe section it was replacing.

The calorimetric method described in the previous section is the operating principle selected for the ash flowmeter. A schematic of the heat exchanger is shown in Fig. 4 and the design specifications for the heat exchanger are given in Table 2. In this design, fifty water-cooled 2.54 cm O.D. bayonet tubes were inserted in the ash recirculation pipe 5 mm apart in a spiral fashion. The use of bayonets instead of tubes extending right through the pipe minimized the number of holes drilled in the ash recirculation pipe and also avoided mechanical problems due to thermal expansion that can occur when a cooling tube is rigidly held at its inlet and outlet of the heat exchanger. It was hoped also that the spiral tube arrangement would interfere negligibly with ash flow and would give a nearly uniform solid exit temperature.

The bayonets were linked to each other by flexible 9.5 mm O.D. (⅜") copper tubing in such a way that the flow of water from one bayonet to another was counter-current to the ash flow. However the fifty bayonets were not all linked in series because the pressure drop at the required water flowrate would have then exceeded the plant's cold water supply pressure. Instead, the bayonets were divided into four groups which operated in parallel as is shown in Fig. 5.

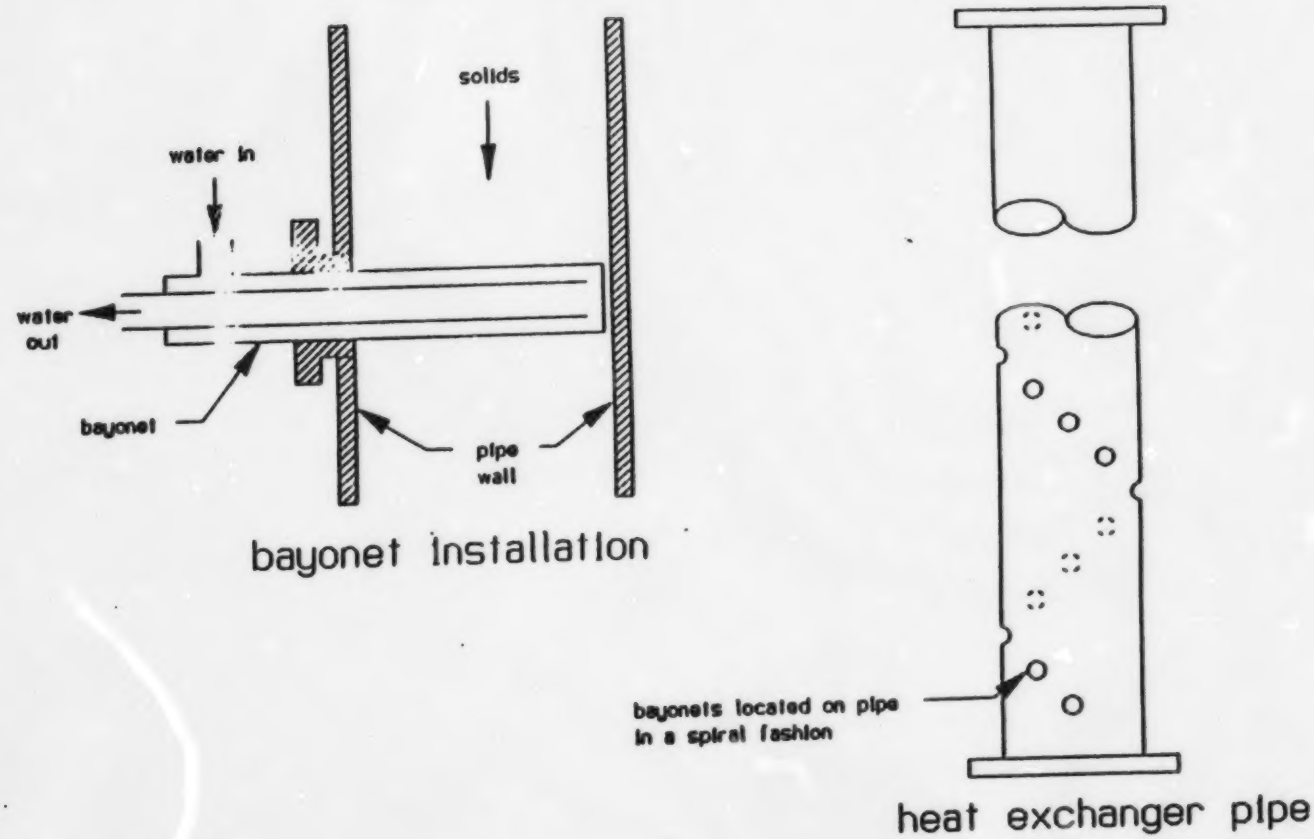

FIG. 4 HEAT EXCHANGER FOR MEASURING ASH RECIRCULATION RATE AT CFB SUMMERSIDE

Table 2. Design Specifications for Ash Flowmeter

Variable		Design value
Ash temperature:	entering	300°C*
	leaving	275°C
Water temperature:	entering	15°C
	leaving	45°C
Ash flowrate		2275 kg/hr*
Heat duty		14 kW
Water flowrate		407 ℓ/hr

* estimates based on plant operating records

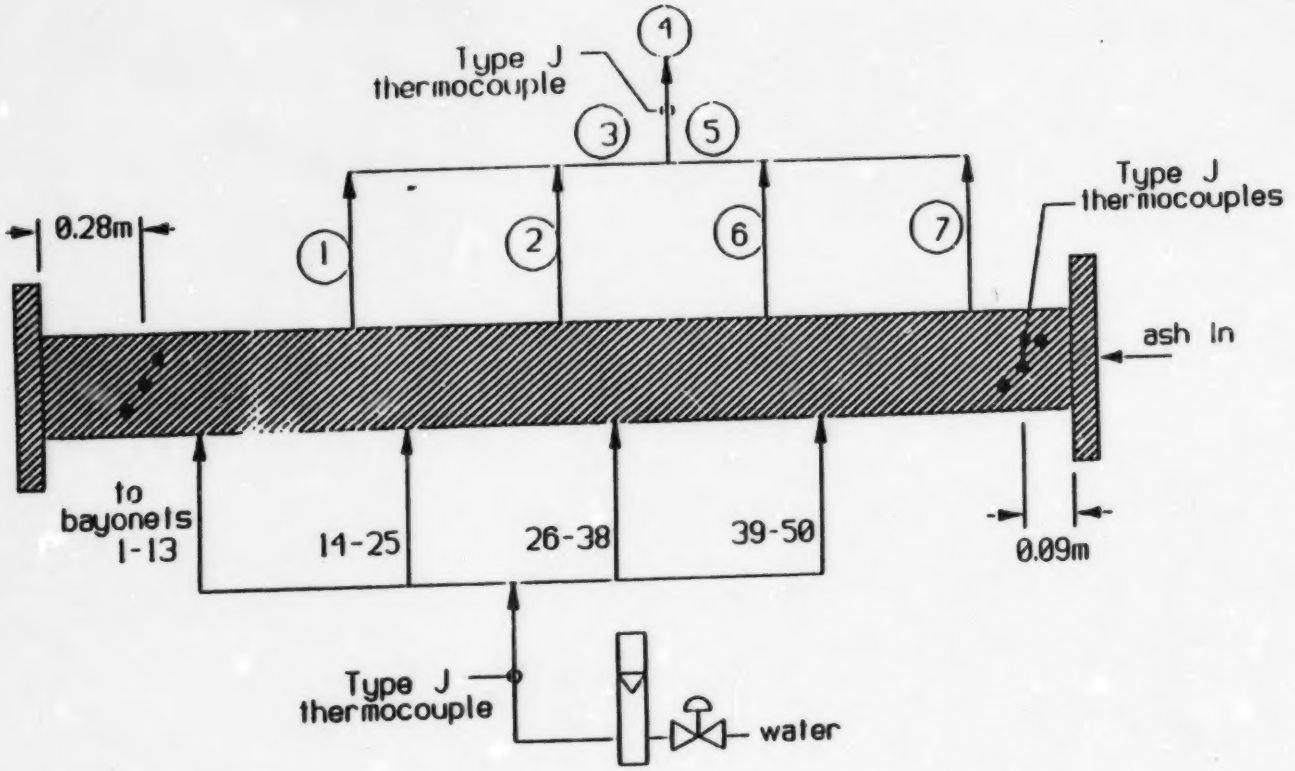

FIG. 5 COOLING WATER DISTRIBUTION WITHIN THE HEAT EXCHANGER

Within a given group the bayonets were linked in series. The flowrate of cooling water was adjusted using a globe valve located upstream of a rotameter on the supply line. Both the inlet and outlet temperatures of the cooling water were measured with sheathed type - J thermocouples inserted in the flowing water.

Three 6.35 mm O.D. (¼") sheathed type-J thermocouples were inserted through the ash recirculation pipe at both ends of the heat exchanger, as shown in Fig. 5, to measure the inlet and outlet temperatures of the ash. At each end of the heat exchanger, the thermocouples were 45° apart as shown in Fig. 6 and were slightly offset in the axial direction as indicated in Fig. 5. This way the thermocouples could be inserted in and out of the pipe to obtain radial temperature traverses of the ash 45° apart. During normal operation of the heat exchanger, the tips of the thermocouples were located at the radial positions indicated in Fig. 6 which are the centers of three concentric regions of equal area. The average of the readings of the three thermocouples so located is a good approximation of the bulk temperature of the ash under plug flow conditions.

Pictures of the assembled heat exchanger are shown in Figs. 7, 8, and 9. Figs. 7 and 8 are respectively side and end views of the heat exchanger with its under side facing up. The two tubes pointing up are the inlet and outlet water lines equipped with tees for mounting the thermocouples. None of the thermocouples had been installed at the time when these pictures were taken but the fittings through which the thermocouples were later inserted can be seen in Figs. 7 and 8. The inside view of the heat exchanger shown in Fig. 9 clearly demonstrates the star arrangement of the bayonets within the heat exchanger.

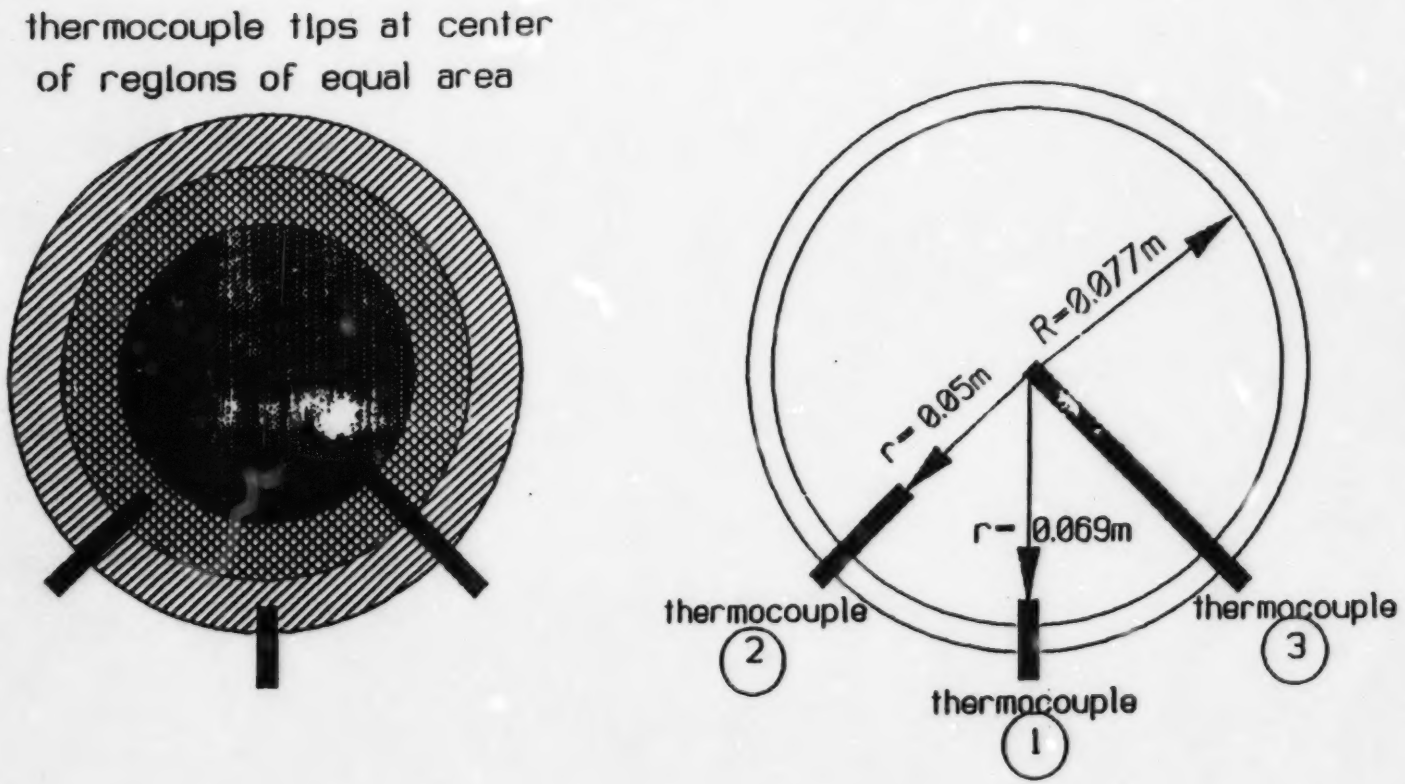

FIG. 6 RADIAL LOCATION OF ASH THERMOCOUPLES

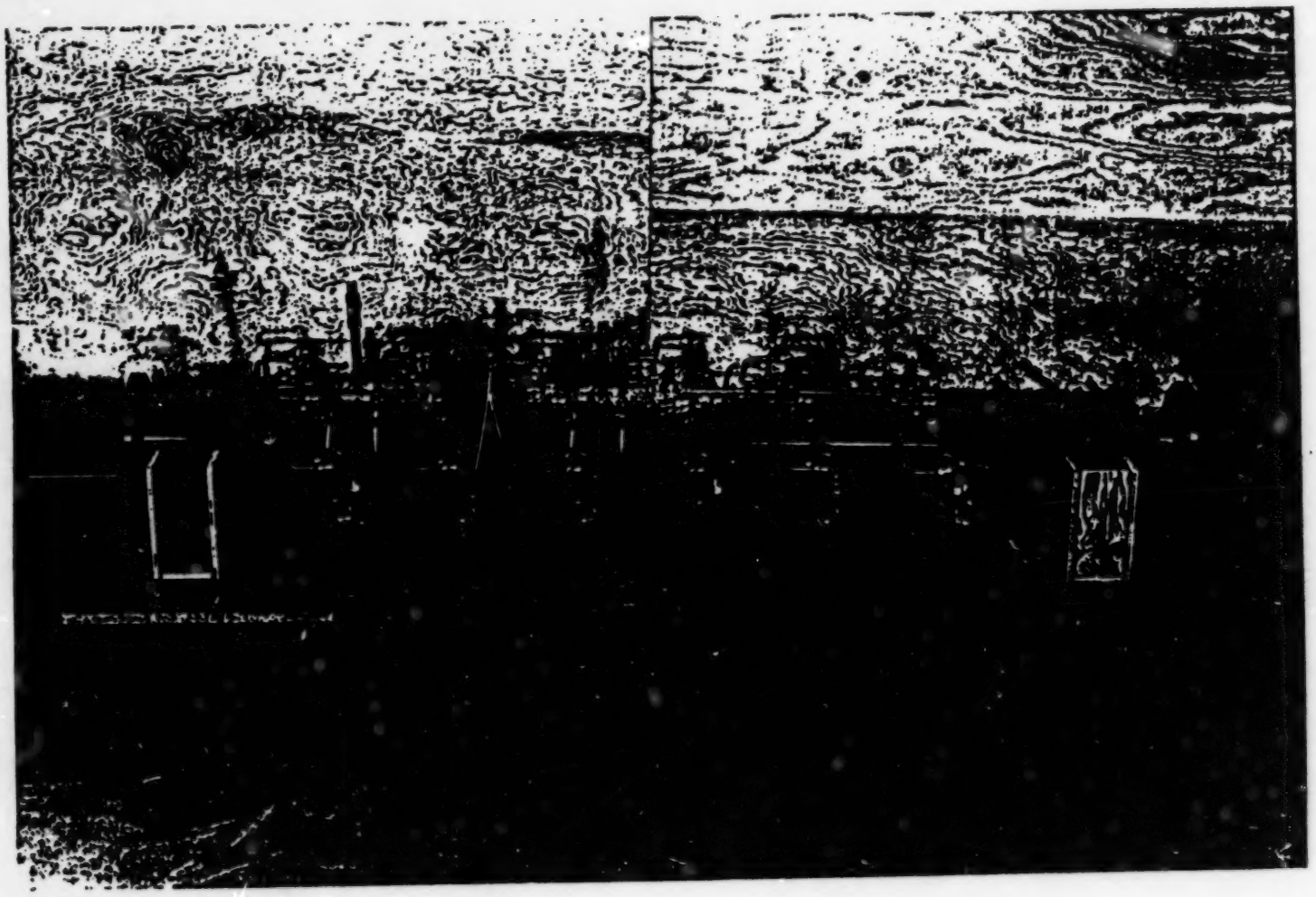

FIG. 7 SIDE VIEW OF THE HEAT EXCHANGER

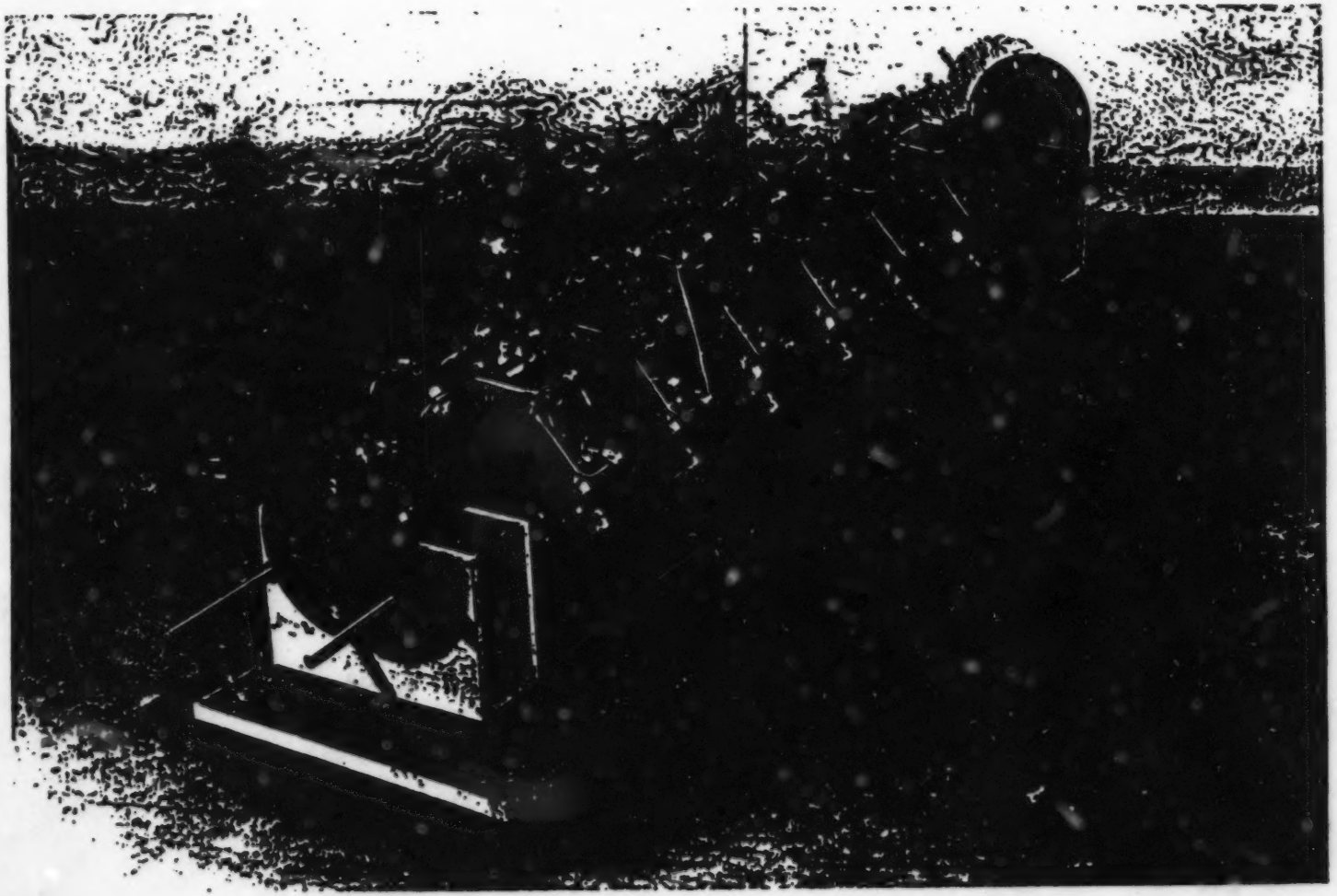

FIG. 8 END VIEW OF THE EXCHANGER

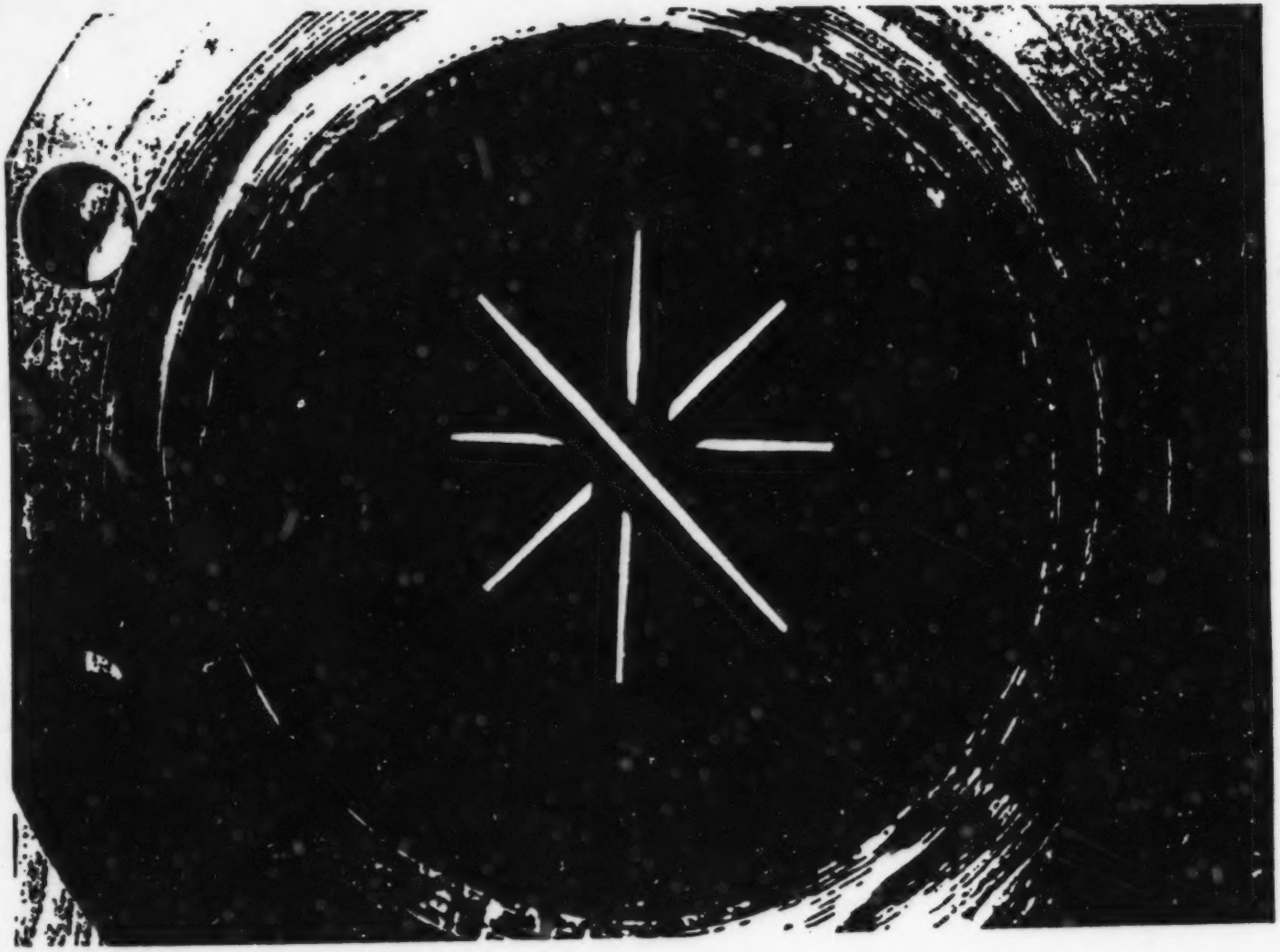

FIG. 9 INSIDE VIEW OF THE HEAT EXCHANGER

4. PROJECT SCHEDULE

The contract for the work described herein was awarded in early June 1990. Soon thereafter a trip was made to the CFB Summerside plant to inspect the location where the ash flowmeter was to be installed and to bring back to UNB for a period of two months the section of pipe that it would replace. This allowed us to build during the summer months an exact replica of the pipe section that would later contain the bayonets. These steps were taken to insure that the installation of the ash flowmeter in the ash re-injection system would be accomplished with minimal problems.

Before finalizing the design of the ash flowmeter, tests were also conducted using the cold fluidized bed model at UNB to measure the heat transfer coefficient between a bayonet and the downward moving solids in the return leg. This was done to insure that the heat exchange surface within the ash flowmeter for the CFB Summerside Plant would be properly sized. The equipment used for these tests is described in the next section.

The construction of the heat exchanger was completed in October 1990 and the ash flowmeter was installed in mid December during a planned shutdown of the No. 2 fluidized bed combustor at CFB Summerside. Normal operation of the boiler resumed soon thereafter and thorough testing of the flowmeter was conducted in early January 1991 while the No. 2 boiler was operating at half load. Another test at full load was attempted in February, 1991 but was aborted because the unit experienced clinkering problems and had to be shut down.

5. HEAT TRANSFER MEASUREMENTS IN THE RETURN LEG OF THE UNB CIRCULATING FLUIDIZED BED

To determine the number of bayonets to be inserted in the ash flowmeter for the CFB Summerside Plant, an estimate of the heat transfer coefficient between a bayonet and a downward moving packed bed of solids had to be obtained. A computerized literature search was conducted but no published data on heat transfer between a horizontal cyclinder and a moving packed bed could be found. Tests were thus conducted using the circulating fluidized bed at the University of New Brunswick.

A schematic of the cold circulating fluidized bed model located in the Chemical Engineering Department at the University of New Brunswick is shown in Fig. 10. The riser or main column is made of sections of 10 cm I.D. plexiglass tubing and has an overall height of 6.1 m. The air entering the column is humidified to minimize the buildup of electrostatic electricity within the unit. The solid particles are fed into the riser via an L-valve and entrained to the top of the unit by the incoming air where they are separated by the primary cyclone before falling back into the downcomer. The solids recirculation rate is adjusted by varying the amount of air injected at the L-valve and measured using the butterfly valve located below the primary cyclone as per technique No. 3 in Table 1. A secondary cyclone followed by a baghouse are used to capture any dust that escapes ~~that~~ the primary cyclone. The return leg of the unit is made of glass sections and has an inside diameter of 15 cm which is very similar to that of the ash recirculation loop at CFB Summerside.

The heat transfer coefficient between a horizontal cylinder and a downward-moving packed bed of solids was determined by inserting instrumented heat transfer probes within the downcomer, 1.56 m above the air injection port on the L-valve. Silica sand having the properties given in Table 3 was used as the

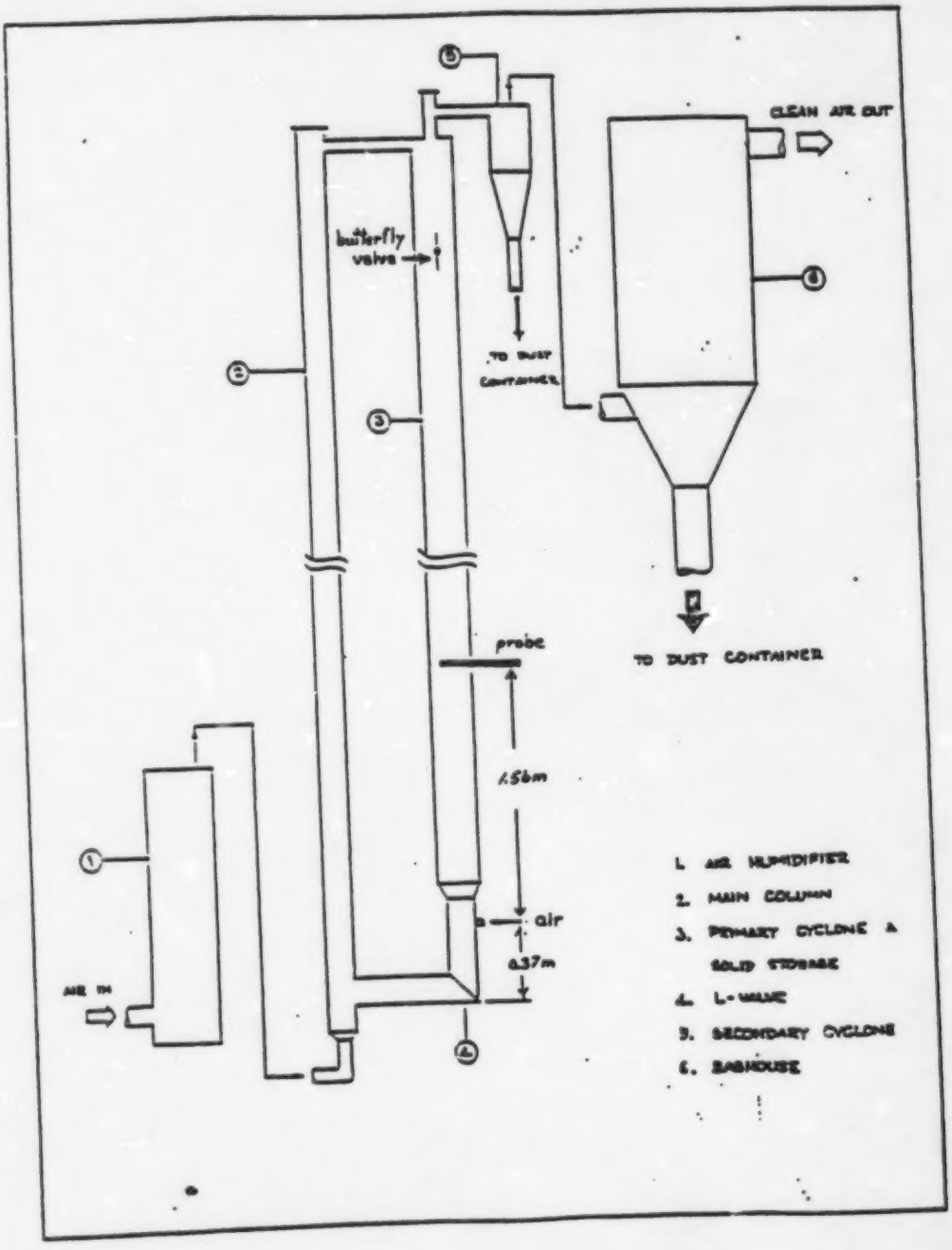

FIG. 10 COLD CIRCULATING FLUIDIZED BED MODEL AT UNB

Table 3. Properties of Sand Material

Mean diameter, μm	290
Bulk particle density, kg/m^3	1486 ± 5
True particle density, kg/m^3	2670
Particle density at minimum fluidization, kg/m^3	1397
Minimum fluidization velocity at 20°C, m/s	0.09 m/s
Bed voidage at minimum fluidization at 20°C	0.49
Angle of repose	35°

solid material in these experiments. Initially one of the bayonets for the proposed ash flowmeter was used as a heat transfer probe and the rate of heat transfer between the bayonet and the solids moving over it in packed-bed mode was determined by running hot water through the bayonet and measuring the temperature drop of the water. The overall heat transfer coefficient based on the exposed surface of the bayonet was calculated as follows:

$$U = \frac{m_w C p_w (T_{w,1} - T_{w,2})}{A (T_{w,avg} - T_s)} \tag{2}$$

where A is the surface area of the bayonet exposed to the solids, T_s is the temperature of the solid particles as measured by a thermocouple immersed in the moving packed bed and $T_{w,avg}$ is the average water temperature taken as the mean of the inlet and outlet water temperatures. The overall heat transfer coefficient takes into account the three modes of heat transfer that operate in series during the transfer of heat from the solid particles to the water:

$$U = \frac{1}{\frac{D_o}{\bar{h}_i D_i} + \frac{D_o \ln (D_o/D_i)}{2k_b} + \frac{1}{\bar{h}_o}} \tag{3}$$

where D_o and D_i are respectively the outside and inside diameters of the bayonet, k_b is the thermal conductivity of the bayonet wall, and $\bar{h}_i$ and $\bar{h}_o$ are the average heat transfer coefficients on the inside and outside of the bayonet, respectively. The first term of the denominator of Eq. (3) is the heat transfer resistance due to convection on the water side, the second term is the resistance due to conduction through the wall and the last term is the resistance due to convection on the solids side. When the first two resistances are much smaller than the third one, as is the case in this study when the water flow is turbulent, then $U = \bar{h}_o$.

Later, two electrically heated probes, one 2.54 cm O.D. (1") and the other 1.27 cm O.D. (½"), were used instead to obtain more precise heat transfer

measurements. These probes were made up of three cylindrical heating sections separated by 6.4 mm long x 1.6 mm thick rings made of 316 stainless-steel, as shown in Fig. 11. Each heating section was built by wrapping nichrome wire around a 19 mm long ceramic tube and covering it with high temperature cement so that the resulting assembly fitted snugly inside a copper tube. The temperature of each heating section was measured with a thermocouple and controlled by varying the voltage applied across the nichrome coil heater. Copper was used for the shell of the heating sections because of its high thermal conductivity, so as to ensure that the outer surface of the heating sections had a uniform temperature.

The air space between the heaters acted as an insulator so that the principal path for heat transfer between the heating sections was by conduction along the stainless-steel rings separating them. When the probes were in use, the temperature of the two end heaters was adjusted slightly above that of the middle heater in such a way that the heat transferred from the end heaters into the stainless steel rings was equal to the heat lost by convection over the surface of the rings. As a result there was no heat loss from the middle heating section to the stainless-steel rings and all the heat generated within the middle section was lost by convection over its surface. It can be shown that this condition is met when

$$T_{end} = (T_{middle} - T_s) \cosh(\bar{a}) + T_s \tag{4}$$

where

$$\bar{a} = \left(\frac{\bar{h}_o}{k_r t (1 + \frac{t}{D_o})} \right)^{1/2} \cdot \ell \tag{5}$$

ℓ, t, D_o and k_r are respectively the length, thickness, outside diameter and thermal conductivity of the stainless steel rings, $\bar{h}_o$ is the average heat

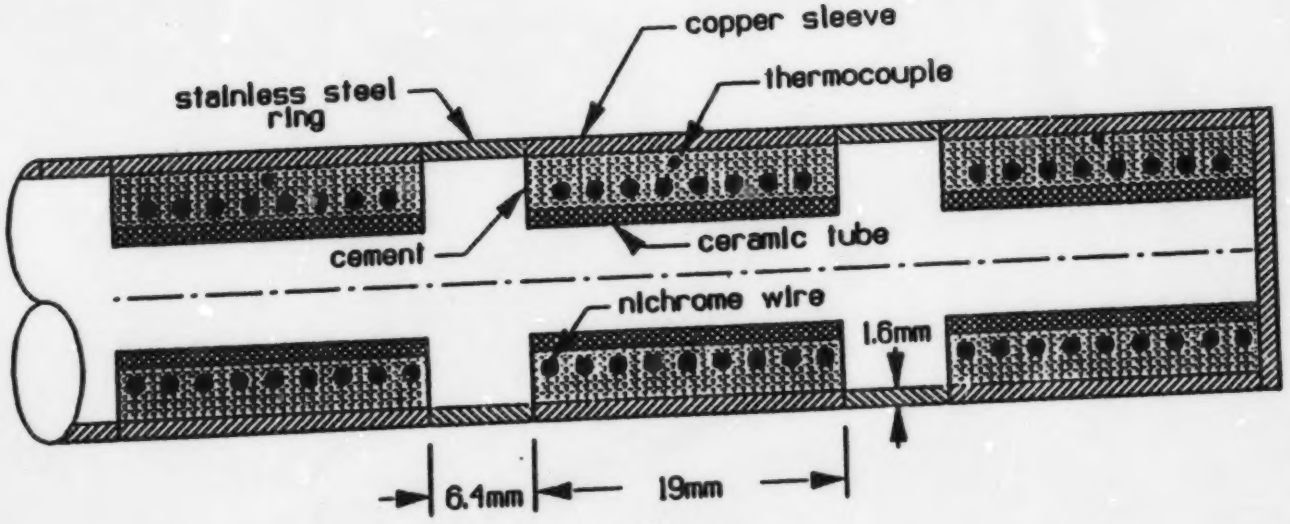

FIG. 11 SCHEMATIC OF THE CYLINDRICAL HEAT TRANSFER PROBE

transfer coefficient over the rings, T_{end} is the temperature of the end heaters and T_{middle} is the temperature of the middle heater. A DC power supply was used for the middle heater so that an accurate determination of the power dissipated could be obtained from voltage and current measurements. All thermocouple readings were recorded by a microcomputer.

The average heat transfer coefficient over the heat flux probe was calculated as follows:

$$\overline{h_o} = \frac{VI}{\pi D_o L (T_{middle} - T_s)} \tag{6}$$

where V is the voltage drop across the middle heater, I is the current supplied to the middle heater and L is the length of the middle heater (=19 mm). The average heat transfer coefficient had to be determined by an iterative procedure whereby $\overline{h}_o$ was initially guessed so that the operating temperature of the end heaters could be determined using Eq. (4), then the true value of $\overline{h}_o$ was calculated from the voltage and current measurements using Eq. (6). If the guessed and calculated values of $\overline{h}_o$ differed by more than 1 $W/m^2 \cdot °C$, then an intermediate value of $\overline{h}_o$ was used as a new guess and the procedure was repeated until satisfactory agreement was achieved. Usually only two or three iterations were required.

The average heat transfer coefficient over a bayonet equipped with circular fins was also determined using the 1.27 cm O.D. electrically heated probe by placing the finned copper sleeve shown in Fig. 12 over the middle heater. To minimize the thermal contact resistance between the sleeve and the copper shell of the middle heater, grease with a high thermal conductivity was spread over the middle heater before sliding the sleeve over it. The average heat transfer coefficient over the finned sleeve was calculated as follows:

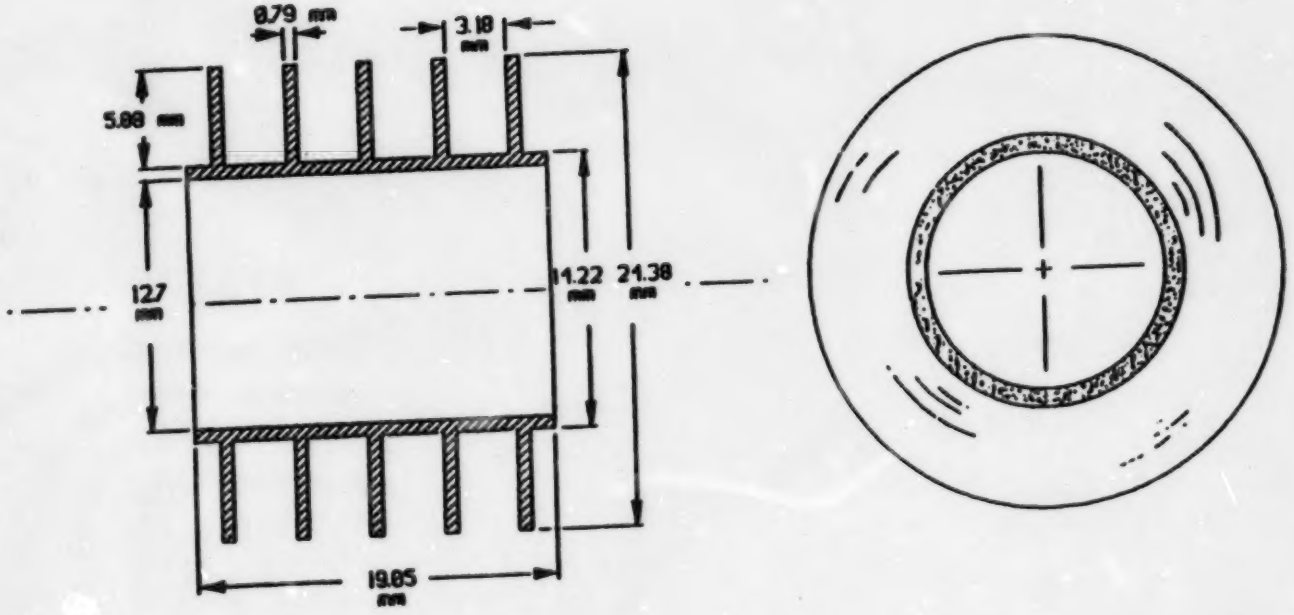

FIG. 12 COPPER SLEEVE EQUIPPED WITH CIRCULAR FINS

$$\overline{h_{fin}} = \frac{VI}{(\eta A_{fin} + A_{cyl})(T_{middle} - T_s)} \qquad (7)$$

where A_{fin} is the total area of the circular fins, A_{cyl} is the area of the exposed cylinder between the fins and η is the fin efficiency. The efficiency of the circular fins is a function of the geometry and thermal conductivity of the fins and of $\overline{h}_{fin}$ (6). During the experiments with the finned sleeve the temperature of the end heaters was determined by assuming that the average heat transfer coefficient over the stainless steel rings was equal to what had been measured under similar operating conditions with the bare probe.

6. RESULTS AND DISCUSSION

6.1 Heat Transfer between a Horizontal Cylinder and a Moving Packed Bed of Sand

The initial tests done in the return leg of the circulating fluidized bed at UNB using one of the bayonets for the proposed ash flowmeter yielded unexpectedly low heat transfer rates. The overall heat transfer coefficient U was about 100 $W/m^2 \cdot °C$ and appeared to be independent of the solids recirculation rate. The estimatesof U obtained using this method were however of poor accuracy because the flowrate of hot water had to be trickled down to 90 cc/min to obtain a drop of 4°C in the water temperature. At this flowrate the water flow was laminar in the bayonet and because of the resulting poor mixing, the thermocouple at the outlet may not have been reading the correct exit bulk temperature.

To obtain more accurate values of the heat transfer coefficient, further measurements were done using electrically heated probes at different solids recirculation rates. The results obtained with the 2.54 cm O.D. and 1.27 cm O.D. probes are plotted in Fig. 13 as a function of the solids flux in the return leg. It can be seen that the $\bar{h}_o$ values obtained with the 2.54 cm O.D. probe are between 130 and 160 $W/m^2 \cdot °C$. These values are about 50% higher than the overall heat transfer coefficients obtained with the bayonet. This difference may be attributed to the inaccuracy of the measurements associated with the bayonet experiment and to the fact that the resistance due to convection on the inside of the bayonet may not have been negligible at the low water flowrates used. The overall heat transfer coefficient U is only equal to $\bar{h}_o$ when the resistance due to convection on the outside is dominant, otherwise U is smaller than $\bar{h}_o$ as can be seen from Eq. (3).

Nonetheless, the $\bar{h}_o$ values obtained were much smaller than what had been anticipated on the assumption that the horizoncal probes were everywhere in contact with moving solid particles. To get a better understanding of the solids

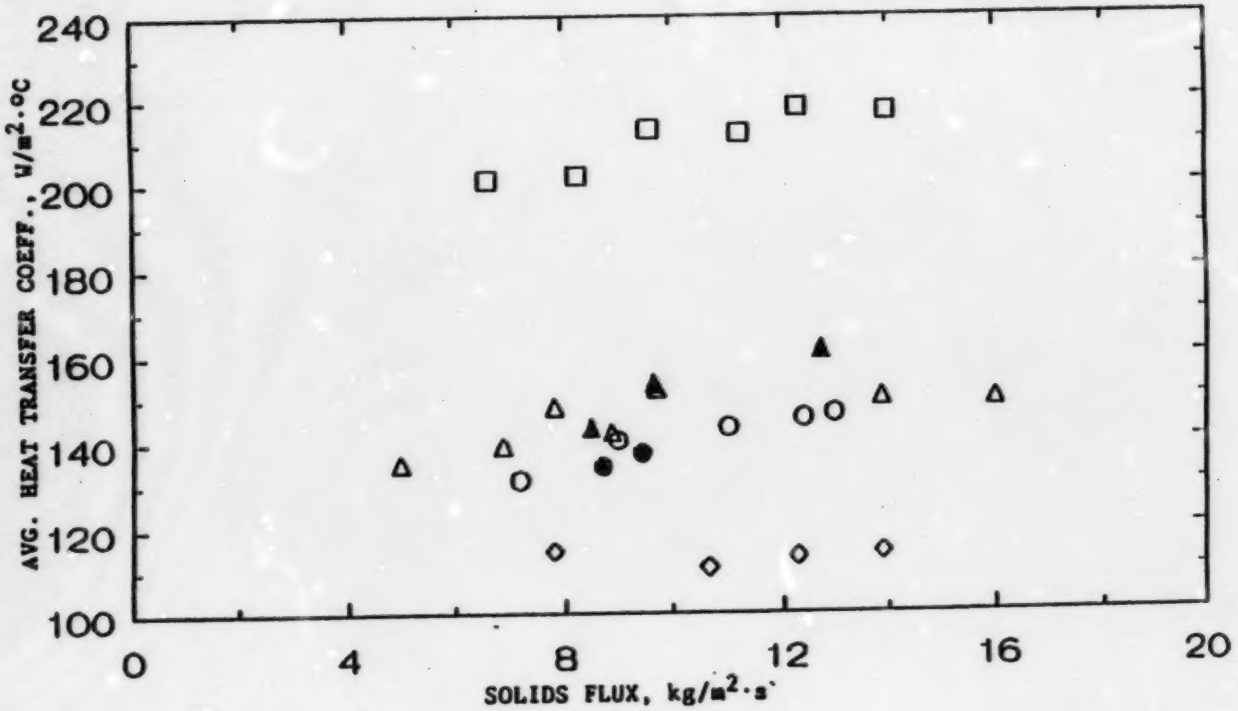

FIG. 13 AVERAGE HEAT TRANSFER COEFFICIENT OVER HORIZONTAL CYLINDERS IMMERSED IN A DOWNWARD MOVING PACKED BED OF SAND. ALL MEASUREMENTS TAKEN AT CENTER OF RETURN LEG WITH A HEAD OF SOLIDS OF 1.4 m UNLESS OTHERWISE INDICATED. □1.27 cm O.D. CYLINDER, ◇1.27 cm O.D. PROBE WITH CIRCULAR FINS, △ 2.54 cm O.D. CYLINDER, ○2.54 cm O.D. CYLINDER WITH 0.4 m HEAD, COLOURED SYMBOLS: MEASUREMENTS TAKEN 3.8 cm OFF CENTER.

flow around the horizontal cylinders, a thin rubber disk was placed at the end of the 2.54 cm O.D. and 1.27 cm O.D. probes and each probe was in turn inserted in the return leg through th normal probe insertion port and pushed in so that the rubber tip was against the glass wall on the opposite side. This way it was possible to observe and film the flow of the solids around the tip of the probes held against the glass.

A schematic of the flow pattern observed around each cylinder is shown in Fig. 14. A nearly stagnant layer of solids in the form of a wedge with an angle of about 50° rested on top of the cylinders whereas an air gap between 0.8 and 1.6 mm thick covered the underside of the cylinders. The sides of the cylinder were intermittently in contact with rising air bubbles and the downward moving packed bed of solids. The air bubbles originated apparently in the air gap below the cylinder and disappeared in the downward moving packed bed of solids before reaching the top of the cylinder. After the passage of each bubble, a wave of downward moving solids rushed against the cylinder and remained in contact with the cylinder until the arrival of the next bubble. Typically, between two and four bubbles went passed the 2.54 cm O.D. probe per second. The presence of air bubbles along the sides of the cylinders was unexpected because the solids in the return leg were not fluidized. However the small stream of air which is percolating up the return leg is evidently able to fluidize the solid particles next to the probes.

The heat transfer rate over a horizontal cylinder immersed in a downward moving packed bed of solids is thus low because only the sides of the cylinder are in contact with fast moving solid particles. The top half of the cylinder is partially insulated by a thick layer of nearly stagnant particles and the lower portion of the cylinder is exposed to an air gap.

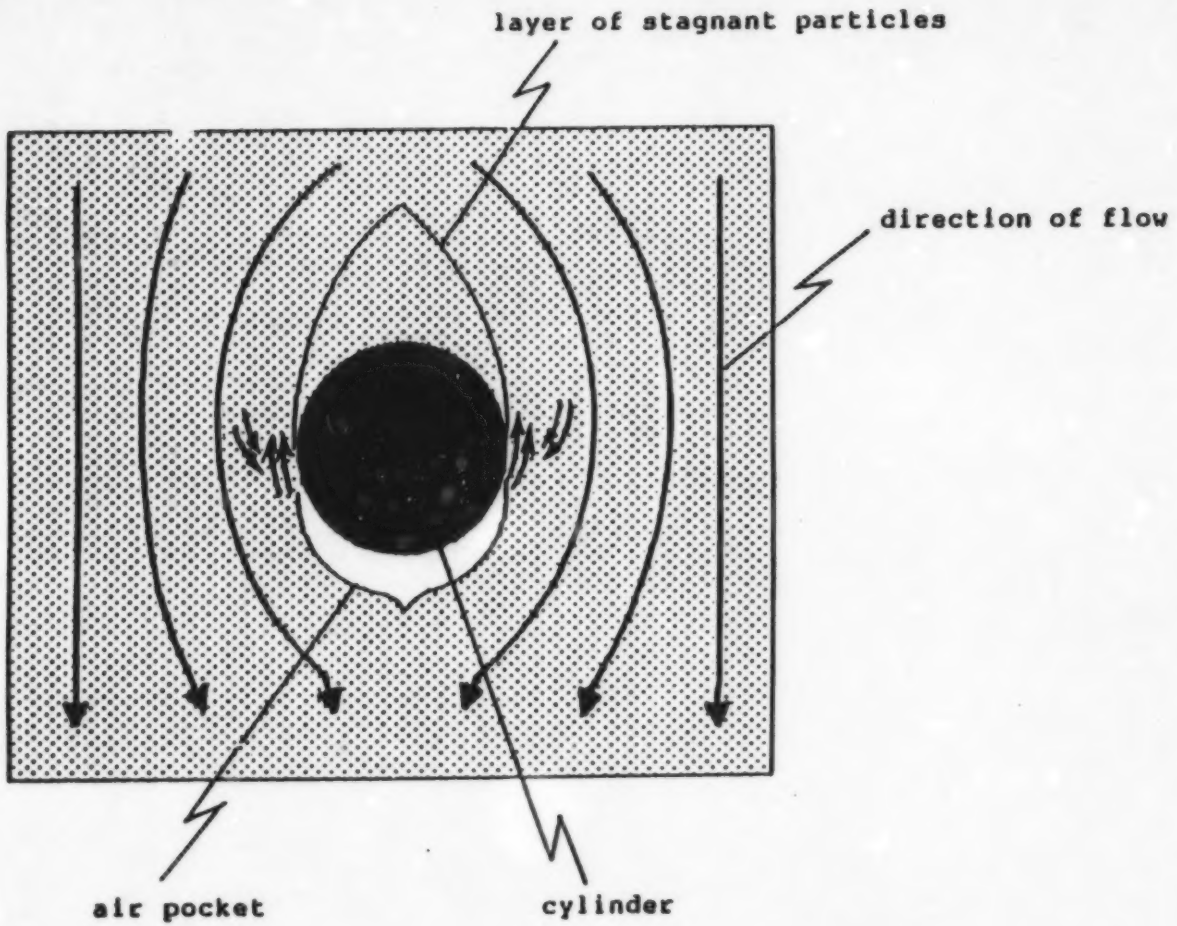

FIG. 14 DOWNWARD FLOW OF SOLID PARTICLES OVER A HORIZONTAL CYLINDER
⟶ SOLIDS FLOW, ⟶ FLOW OF AIR BUBBLES

It can also be seen in Fig. 13 that the average heat transfer coefficient over the 2.54 cm O.D. probe decreased slightly when the head of solids above the probe was lowered. The head of solids in the return leg was decreased by draining solid particles from the system. It should be pointed out that the head values quoted in Fig. 13 were obtained under static conditions. Under dynamic conditions, the head of solids above the probe decreased slightly with increasing solids recirculation rate because of the increasing solids hold-up in the riser. Because of the configuration of the recirculating loop, the pressure drop across the riser and the return leg must be equal and independent of the solids inventory in the return leg at a given solids recirculation rate and superficial velocity in the riser. For the pressure drop to stay the same, the flowrate of air percolating up the return leg of solids must increase as the solids inventory is decreased and as a result the time fraction that the sides of the probes are covered with air bubbles might increase with the decreasing head of solids. This may explain why the average heat transfer coefficient decreases slightly with solids head.

It is interesting also to note in Fig. 13 that for both the 2.54 cm O.D. and 1.27 cm O.D. probes, the heat transfer coefficient increases only slightly with solids flux. This is surprising because it had been anticipated that the contact time of the particles with the probes would decrease with increasing solids flux and the heat transfer coefficient would increase as a result. It thus appears that the frequency of bubble passage along the sides of the cylinder is the only controlling factor affecting contact time of the particles. Further work is however required to confirm this.

Of all the variables examined in this study, the probe diameter is the one having the most influence on the heat transfer coefficient as can be seen in Fig. 13. The average heat transfer coefficient over the 1.27 cm O.D. probe being

about 40% larger than that of the 2.54 cm O.D. probe. It is unclear if this is because a larger fraction of the 1.27 cm O.D. probe is exposed to fast moving solids or because the contact time of the solids with the 1.27 cm O.D. probe is shorter. Further work is also required to elucidate this question.

The rate of heat transfer from the probe with circular fins was about three times that obtained with the plain 1.27 cm O.D. probe although the total exposed area of the fins (4.058×10^{-3} m^2) was about five times larger than that of the plain probe. As a result the average heat transfer coefficient for the finned probe was lower than that of the plain probes, as can be seen in Fig. 13. This is probably because the flow of solids over the finned probe was hindered by the presence of the fins. The fin efficiency used in Eq. (7) was calculated using the correlation for circular fins reported by Incropera and DeWitt (6). In all cases the fin efficiency was very close to 100% because of the low value of $\bar{h}_o$ and the high thermal conductivity of the copper fins; i.e. the temperature of the fins was essentially everywhere equal to the probe temperature.

To determine if the heat transfer coefficient was a function of lateral position in the riser, measurements were also taken with the 2.54 cm O.D. probe at off-center positions. It can be seen in Fig. 13 that the average heat transfer coefficient within the 15 cm I.D. downcomer is essentially independent of radial position within a region of plus or minus 3.8 cm of the center. This may be an indication that the solid particles move in plug flow in the center of the downcomer. However to verify whether plug flow conditions were present over the full width of the return leg, particle velocities near the glass wall were determined by timing the descent of identifiable particles as a function of solids flux. The results are presented in Fig. 15. The average solids flux in these experiments was determined by dividing the solids recirculation rate measured using the butterfly valve by the cross-sectional area of the downcomer.

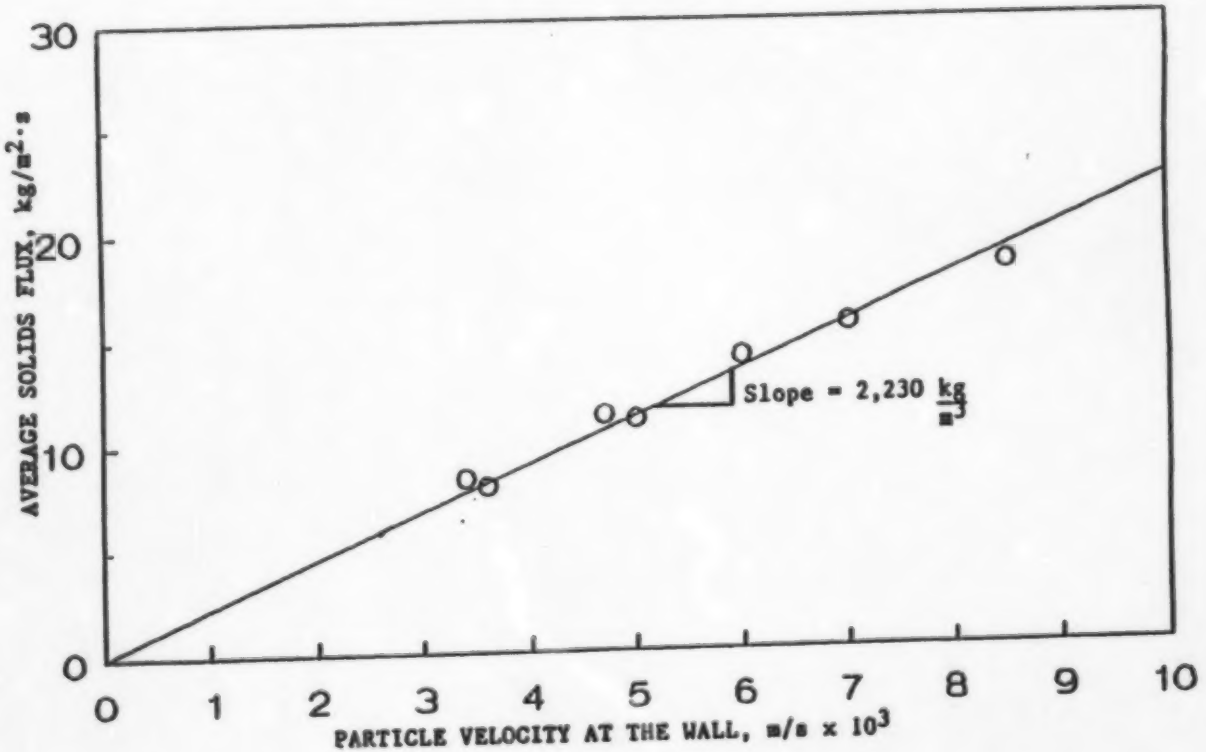

FIG. 15 SOLIDS FLUX IN THE DOWNCOMER VERSUS PARTICLE VELOCITY NEXT TO THE WALL

Under plug flow conditions the local solids flux is everywhere equal to the average solids flux. The relationship between solids flux and particle velocity at any given position is

$$F = \rho u \tag{8}$$

where F is the local solids flux, ρ is the local density of the solids and u is the particle velocity. As can be seen in Fig. 15, the relationship between the average solids flux and the particles' velocity at the wall is linear as predicted by Eq. (8) but the slope of the straight line, ρ, is 2,230 kg/m^3 which cannot be the density of the sand next to the wall since the bulk density of the sand under static conditions is 1486 kg/m^3, as reported in Table 3. This indicates that the flux of solids next to the wall must be much less than the average solids flux and that plug flow conditions do not prevail near the wall. The linear relationship in Fig. 15 must then have been obtained because the flux near the wall and the average solids flux are linearly dependent.

Based on the results of Fig. 13, the following number of 15 cm long heat exchange tubes would have to be installed in the ash flowmeter to meet the specifications given in Table 2: fifteen finned bayonets, or thirty two 2.54 cm O.D. bayonets, or forty three 1.27 cm O.D. bayonets. The difference between the number of finned bayonets and that of 2.54 cm O.D. bayonets was not however considered large enough to warrant the tedious manufacture of bayonets with circular fins. It was then decided to build the ash flowmeter with plain 2.54 cm O.D. bayonets and to use 50 of them instead of 32 as a safeguard because the return leg at CFB Summerside is sloped instead of being vertical like the one at UNB and because it was unknown whether the ash material would behave like the sand used at UNB.

6.2 PERFORMANCE OF THE ASH FLOWMETER

The operation of the ash flowmeter was tested at CFB Summerside on January 7, 8 and 9, 1991. The results of these tests are presented hereafter. During the tests, boiler No. 2 was operated at half load and conditions were stable.

The particle size distribution of the ash flowing through the heat exchanger on January 8, 1991 is presented in Fig. 16 together with the particle size distribution of the silica sand used in the circulating fluidized bed unit at UNB. It can be seen that the ash was finer (d_{50} = 50 μm) and had a wider particle size distribution than the sand used for the heat transfer studies at UNB. The ash was also much lighter than the sand; it had a true density of 1,380 ± 110 kg/m^3 and a bulk density of 879 ± 43 kg/m^3. The elemental composition of the ash as determined by EMR is given in Table 4. The molecular composition also given in Table 4 was obtained by assuming that Si, Al and Fe were present in the ash in the form of their normal oxides, S was present as $CaSO_4$, the Ca not tied up as $CaSO_4$ was present as CaO and the carbon content was equal to the loss on ignition.

The following six compounds: SiO_2, Al_2O_3, Fe_2O_3, $CaSO_4$, CaO, and C, constitute about 95% of the ash as can be seen in Table 4. For the purpose of estimating the heat capacity of the ash, the ash was assumed to be composed of only those six components and to behave as an ideal solution, i.e. the heat capacity of the ash components was assumed to be that of the pure compounds. The heat capacity of the ash estimated in this manner is 0.84 kJ/kg·°C as shown in Table 5. For the purpose of this calculation, the weight fractions of the six ash components were adjusted slightly while keeping the relative concentration of the components the same, so that the sum of the mass fractions would equal unity. The error in estimating the heat capacity by this method is expected to be small because the heat capacity per unit weight is about the same for all

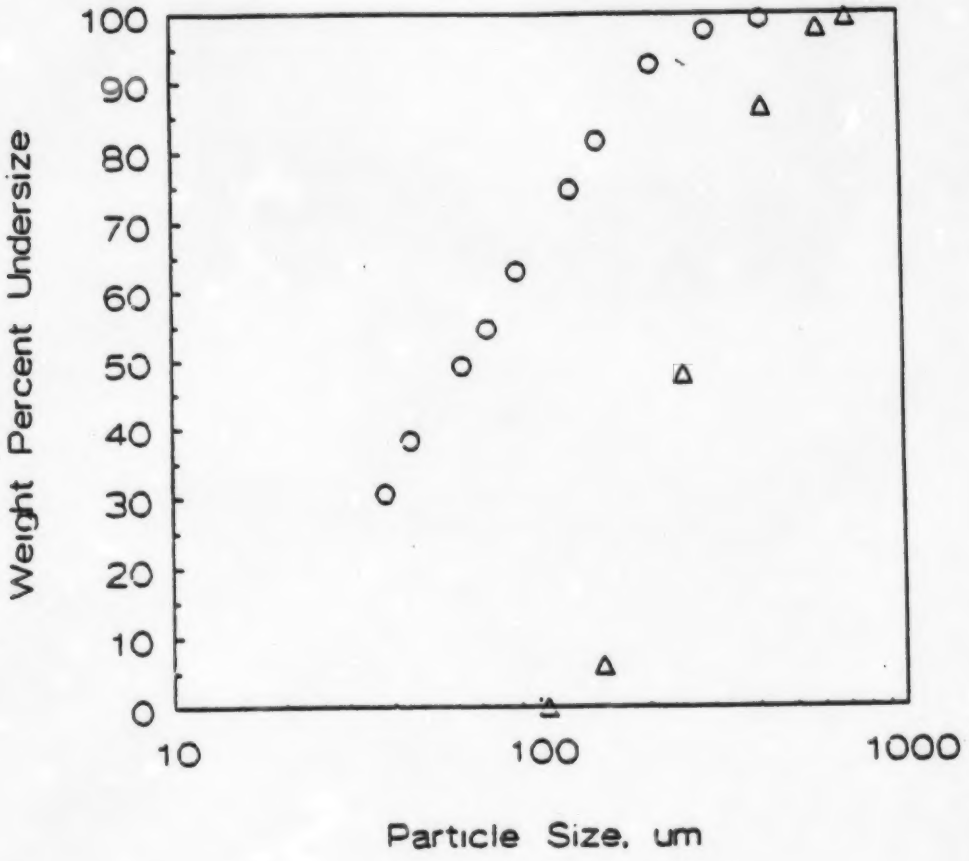

FIG. 16 PARTICLE SIZE DISTRIBUTIONS OF THE CYCLONE ASH FROM CFB SUMMERSIDE AND SAND IN THE CIRCULATING FLUIDIZED BED AT UNB. △ SILICA SAND, ○ ASH.

TABLE 4. CHEMICAL COMPOSITION OF THE CYCLONE ASH FROM CFB SUMMERSIDE

Elemental	Composition wt%	Molecular	Composition wt%
Si	4.85	SiO_2	10.39
Al	2.00	Al_2O_3	3.78
Fe	8.42	Fe_2O_3	12.03
Ti	0.07	$CaSO_4$	34.08
P	0.06	CaO	18.66
Ca	23.35	C	15.7
Mg	0.26	other	5.36
S	8.02		Σ = 100
Na	0.44		
K	0.18		
Ba	0.04		
Sr	0.02		
LOI[1]	15.7		
AI[2]	13.7		

[1] loss on ignition ; [2] acid insolubles

TABLE 5. HEAT CAPACITY OF CYCLONE ASH

Compound	Heat Capacity, Cp[1] kJ/kg·°C (80 - 180 °C)	Approximate weight fraction, x
SiO_2	0.9	0.11
Al_2O_3	1.0	0.04
Fe_2O_3	0.75	0.13
$CaSO_4$	0.80	0.36
CaO	0.80	0.20
C	1.0	0.16
		1.0

$$Cp_{ash} = \sum_{i=1}^{6} x_i \, Cp_i = 0.84 \ kJ/kg \cdot °C$$

[1] from ref. (8)

solid components and thus the calculated heat capacity of the ash is not very sensitive to the ash composition used.

The results of the tests conducted at CFB Summerside using the ash flowmeter are summarized in Table 6. During each test, the ash and water temperatures were read between ten and fifteen times at about one minute intervals; the average of these temperature readings is reported in Table 6. The flowrate of water was continuously monitored using a rotameter to ensure that the flow was steady and a bucket and stop watch were used two to three times during each test to obtain a precise water flowrate measurement. The average ash inlet and outlet temperatures reported in Table 6 are the means of the readings obtained with thermocouples 1, 2, and 3. Refer to Fig. 6 for the radial position of thermocouples 1,2 and 3. The calculated ash flowrate was obtained using Eq. (1) and by assuming that the bulk temperatures of the ash were equal to the average temperatures given in Table 6 and that the heat capacity of the ash during each test was equal to the estimate obtained in Table 5. As can be seen in Table 6, the calculated ash flowrate varied from test to test but was generally between 540 and 630 kg/hr.

During some tests the ash flowrate was also determined directly by momentarily diverting the ash stream flowing through the heat exchanger into a barrel. The ash drain line located on the J valve (see Fig. 3) was used for this purpose during trials 4 and 5. However the ash flowrates obtained during these two tests are believed to be erroneous because the air to the J-valve had to be left on for the ash to flow out of the return pipe into the barrels and as a result it is unknown whether all the ash was collected or if some entered the combustor. Furthermore it is unknown whether the inventory of ash in the return pipe stayed constant while the drain line at the J valve was opened. More accurate ash flowrate measurements were taken during trials 7 and 10 using the

TABLE 6. RESULTS OF TEST PERFORMED ON ASH FLOWMETER

Trial #	Date	Time	Water Flowrate ℓ/min (±0.1)	Water Temp. °C		Ash Inlet Temp., °C (±2)				Ash Outlet Temp., °C (±4)				Ash Flowrate, kg/hr		Q kW
				In(±0.1)	Out(±0.4)	T1	T2	T3	T_{ave}	T1	T2	T3	T_{ave}	calculated	measured	
1	Jan.7,1991	16:00	8.5	8.7	25.0	105	142	166	138	80	95	125	100	910	-	9.7
2	Jan.8,1991	9:25	8.7	8.8	18.3	140	162	174	159	129	131	135	132	920	-	5.8
3		10:00	9.1	8.7	17.0	157	170	180	169	135	129	136	133	630	-	5.3
4		10:20	9.3	8.5	18.9	152	167	176	165	110	114	117	114	570	283[2]	6.7
5		11:30	9.2	8.5	15.6	131	152	167	150	126	124	127	126	810	352[2]	4.5
6		15:00	9.3	8.4	17.3	151	166	175	164	121	118	124	121	580	-	5.8
7	Jan.9,1991	12:15	8.8	9.5	24.2	-	165	175	170	80	98	120	98	540	445,530,432[3]	9.0
8		13.15	8.7	9.9	24.4	-	164	173	169	78	103	118	100	550	-	8.8
9		15:00	8.9	9.5	24.9	170[1]	160	172	167	89	92	110	97	590	-	9.6
10		15:30	8.9	9.5	24.3	168[1]	154	169	164	83	89	111	94	570	382,382,400[3]	9.2
11		16:45	9.0	9.5	18.3	160[1]	135	173	156	96	115	140	117	610	-	5.5

[1] thermocouple tip moved in 4 cm from its normal position
[2] measured using bottom drain line
[3] measured using top drain line

ash drain line below the cyclone hopper (refer to Fig. 3). During these two tests the ash flowrate measurements were done as follows:

i) the air to the J-valve was first turned off to let the ash level in the return pipe buildup passed the inlet of the drain line below the cyclone hopper,

ii) the valve on the drain line was opened and the material that had accumulated above the valve fell into a drum,

iii) the valve was then closed and the stop watch started while an empty barrel was located below the drain line,

iv) the valve was then re-opened and ash was collected in the barrel for a period of about 3 minutes,

v) steps iii) and iv) were then repeated two more times to get a total of three ash flowrate measurements.

In both trials 7 and 10, the calculated ash flowrate exceeded the measured value; in trial 7, it was 13% higher whereas in trial 10 it was 31% higher. Nonetheless, the agreement is good considering the approximations that had to be made in the calculation of the ash flow. The reasons for the discrepancy are discussed below.

The measurements of the ash flowrate using the top drain line were fairly reproducible and are believed to be accurate. It is unlikely that any ash entered the combustor while the air to the J valve was turned off. However it is not known for certain that the split of the recycled ash between the two return legs stayed the same after the air to one J valve was turned off. At CFB Summerside, there is no measurement of the amount of air injected at the J-valves nor any measurement of the fraction of the injected air flowing up the ash return pipes. As will be explained below, the flow of air up the ash return pipes may not be negligible.

To determine whether the ash was flowing in packed bed mode at the inlet of the heat exchanger, a 0.95 cm O.D. (3/8") tube was introduced in the return pipe through the port for inlet thermocouple no. 2. When the tube was first introduced in the pipe a strong and steady flow of ash escaped through its opened end indicating that the tip of the tube was within a zone of high solids loading. Ash kept on coming out as the tube was pushed in until the tip of the tube was 4.4 cm from the top of the return pipe; from that point on, only gases escaped from the tube. Two scenarios are proposed in Fig. 17 to explain the existence of the zone void of solids that was found near the top of the return pipe. It is highly unlikely that the top of the moving packed bed was located in line with the point of entry of the tube as is suggested in scenario A. Instead it is much more probable that ash was moving in packed bed mode along the bottom of the return pipe and air was flowing up through a 4.4 cm gap along the top of the ash return pipe as suggested in scenario B. O'Dea et al.[7] have recently reported that this type of channelling flow does indeed occur in inclined fluidized beds. For fluidized beds inclined at 45°, the air channel develops at a superficial air velocity equal to about half the minimum fluidization velocity. Hence, it is apparent that the flow of ash down the inclined return pipe at CFB Summerside is not like the piston flow observed in the vertical downcomer of the circulating fluidized bed at UNB and as a result, a lot more air is probably flowing up the return pipe at CFB Summerside.

Presumably the upflowing air gained heat during its passage through the heat exchanger because it was flowing counter-current to the ash. Both the heat lost to the upflowing air and to the surroundings were neglected in the ash flow calculations. These omissions should result in an underestimate of the ash flowrate as can be seen from inspection of the general heat balance equation:

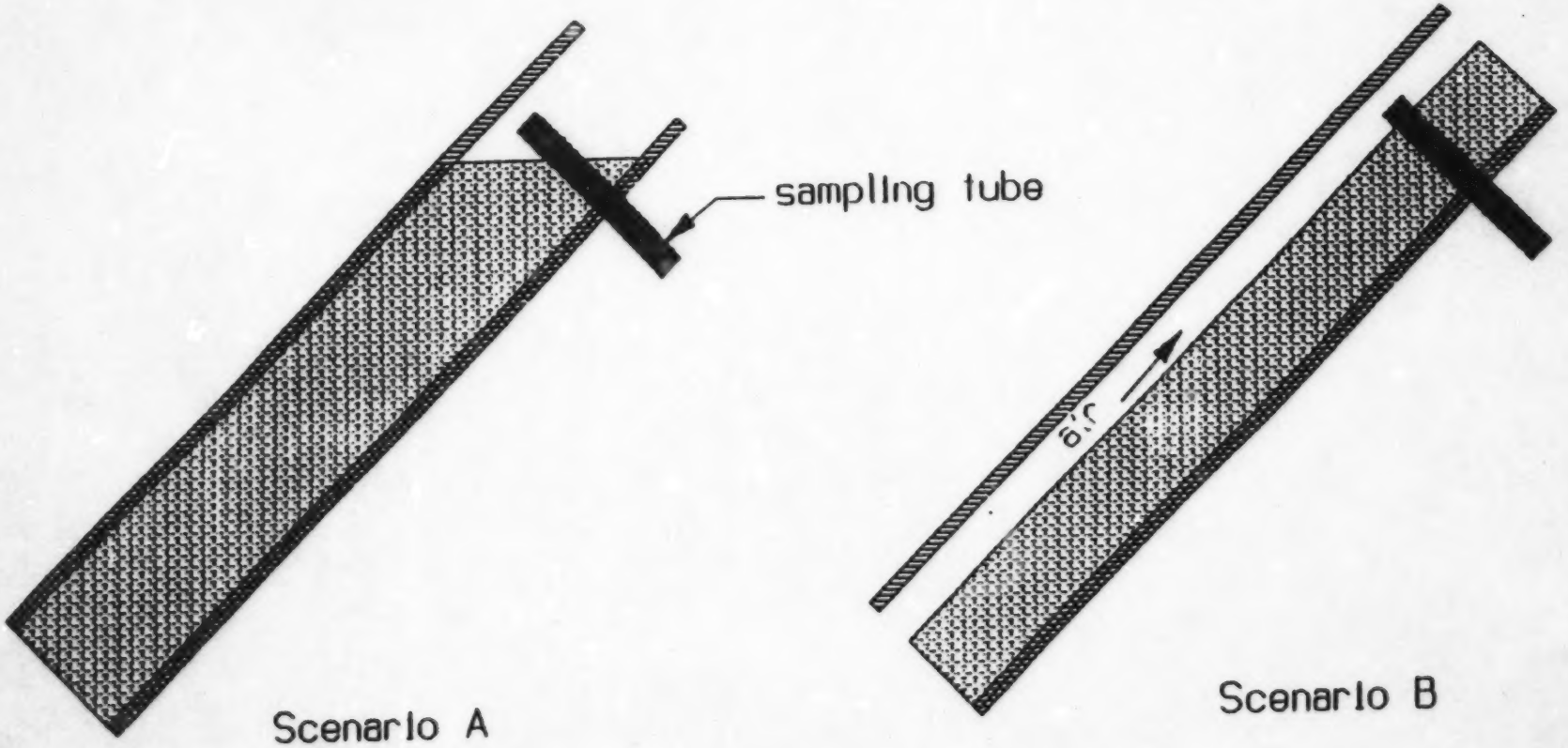

FIG. 17 POSSIBLE ASH FLOW PATTERNS IN RETURN PIPE

$$m_s = \frac{m_w C_{pw} (T_{w,2} - T_{w,1}) + \text{heat transferred to surroundings} + \text{heat gained by upflowing air}}{C_{ps} (T_{s,1} - T_{s,2})} \quad (9)$$

and thus do not explain why the calculated ash flow exceeded the measured flow. During the design stage, it was decided not to insulate the heat exchanger because it was estimated that the heat loss from the bare exchanger to the surroundings would be less than 1 kW. Although this is small compared to the heat picked up by the water (see Table 6), it is not totally negligible and in retrospect, it is apparent that the heat exchanger should have been insulated.

It had been hoped that the ash temperature at the outlet of the heat exchanger would be nearly uniform because of the spiral distribution of the bayonets. Such was the case for all tests conducted on January 8 as can be seen in Table 6 but on January 7 and 9, the ash outlet temperature was highly non uniform. On those latter days, the outlet ash temperature was highest at the center of the pipe and lowest at the wall and the profile could not be changed by modifying the air distribution at the J-valve. More surprising, however, were the large radial variations in the measured ash inlet temperature reported in Table 6. It had been expected that ash would be of uniform temperature at the inlet of the heat exchanger because of the good solids mixing that takes place in the cyclone. However the temperature traverse obtained on January 7 and shown in Fig. 18 clearly indicated that the heat loss from the ash to the surroundings along the pipework between the cyclone and the heat exchanger was significant. Before doing any test on January 8, the section of return pipe between the hopper below the cyclone and the heat exchanger was insulated. Although the addition of insulation did not eliminate the inlet temperature gradient, it reduced it significantly as can be seen in Table 6 and Fig. 17.

Because of the radial and circumferential variations in the outlet and inlet ash temperatures, an error was introduced in the calculation of the ash

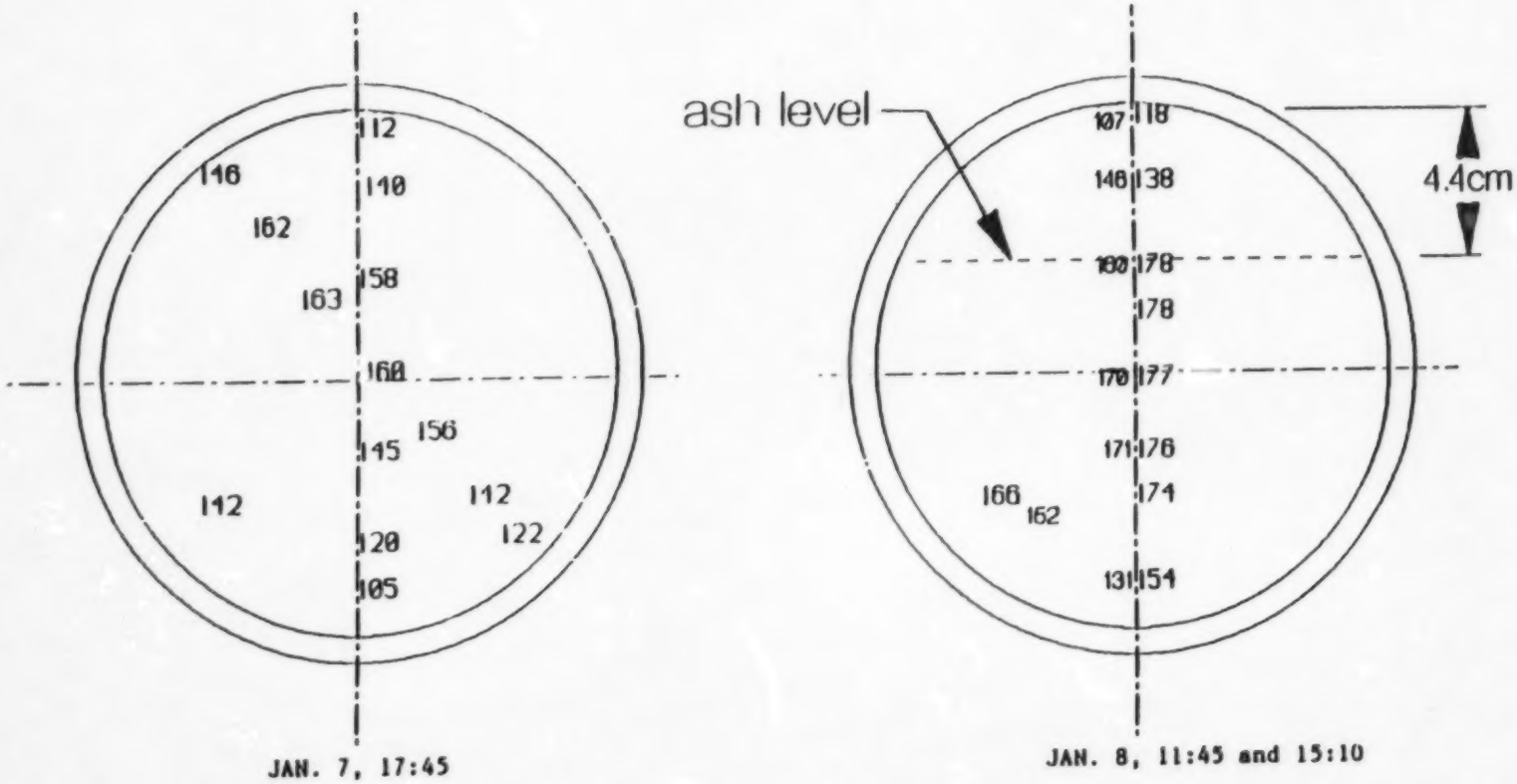

FIG. 18 TEMPERATURE DISTRIBUTION OF THE ASH AT THE HEAT EXCHANGER INLET (°C)

flowrate by assuming that the bulk inlet and outlet temperatures of the ash were equal to the average temperatures given in Table 6. The bulk temperature of the ash is only equal to the average temperature of thermocouples 1, 2 and 3 when plug flow conditions prevail and there are no circumferential temperature variations, otherwise

$$T_{bulk} = \frac{\int_0^R \int_0^{2\pi} F_s T_s r \rho \, d\theta \, dr}{m_s} \quad (for\ constant\ C_p) \tag{10}$$

and a knowledge of F_s and T_s as a function of position is required to calculate T_{bulk}. The plug flow approximation is a great oversimplification in this case not only because F_s is lower near the wall as discussed in Section 6.1 but also because F_s is zero over a significant region within the top half of the return pipe as shown in Figs. 17 and 18. It is thus believed that the discrepancy between the measured and calculated ash flows in Table 6 is mainly due to the inaccuracy of the bulk temperature estimates.

By comparing the experimental results of Table 6 with the design specifications for the ash flowmeter in Table 2, it can be seen that both the ash flowrate and ash inlet temperature were grossly overestimated during the design stage. The heat exchanger performed well in spite of these unexpected results because the heat exchange area had been oversized to counteract such unforeseen events, as explained in Section 6.1.

Three tests were also conducted to determine the overall heat transfer coefficient for each of the four bayonet bundles in the heat exchanger; these results are presented in Table 7. In these tests, the outlet water temperature was determined at the seven positions indicated in Fig. 5 by pressing a fine type-K thermocouple against the outside surface of the copper conduits using a piece of styrofoam insulation. By assuming that the water flow was equally

divided between the four bundles and by neglecting heat losses to the surroundings and upflowing air, it was possible to calculate from a heat balance the bulk ash temperature at the exit of each bundle. The overall heat transfer coefficient for each bundle was then obtained using

$$U = \frac{m_w C_{pw} (T_{w,2} - T_{w,1})}{nA (T_s - T_w)_{avg}} \qquad (11)$$

$$\text{where} \quad (T_s - T_w)_{avg} = \frac{(T_{s,1} - T_{w,2}) + (T_{s,2} - T_{w,1})}{2} \qquad (11)$$

and where n is the number of bayonets in the bundle, A is the surface area of one bayonet, m_w is the flowrate of water in the bundle, and the subscripts 1 and 2 refer to conditions at the inlet and outlet of the bundle, respectively.

In all tests the overall heat transfer coefficient was highest in the bundle containing bayonets 1 to 13 and lowest in the bundle containing bayonets 26 to 38. Furthermore, ~~although~~ the values of the overall heat transfer coefficient obtained in tests 1 and 3 ~~are~~ very similar, they are much higher than those obtained in testt 2. These spatial and temporal variations in U were probably caused by similar variations in the solids loading within the heat exchanger, but no attempt was made to experimentally verify this hypothesis. It is also interesting to note that despite the air channelling in the return pipe at CFB Summerside, the values of the heat transfer coefficient reported in Table 7 are similar to those measured in the downcomer of the circulating fluidized bed at UNB (see Fig. 13). This is probably because the negative impact of air channelling on the overall heat transfer coefficient was compensated by the fact that the ash at CFB Summerside was finer than the sand used at UNB. In fluidized beds, the heat transfer coefficient due to solids convection generally increases with decreasing particle size (9).

TABLE 7. OVERALL HEAT TRANSFER COEFFICIENT OVER EACH BAYONET BUNDLE

Test #	Date	Time	Water Flowrate ℓ/min	Inlet Water Temp., °C	Outlet Water Temperatures, °C							Ash Temp. °C		U over bayonets, W/m²°C			
					T1	T2	T3	T4	T5	T6	T7	In	Out	1-13	14-25	26-38	39-50
1	Jan.7,1991	17:00	8.5	8.7	25.6	21.3	24.0	22.4	21.7	20.7	21.7	138	100	170	130	100	120
2	Jan.8,1991	15:30	9.3	8.4	19.0	16.1	16.7	17.7	17.6	15.7	19.6	164	121	90	70	50	90
3	Jan.9,1991	12:40	8.7	9.9	28.0	23.1	25.8	25.2	24.0	22.9	25.0	170	98	200	130	100	110

7. CONCLUSION

The ash flowmeter developed for the No. 2 fluidized bed boiler at CFB Summerside performed well and had no apparent negative impact on the operation of the solids recirculation loop of the unit. At half load, the ash flowrate through the flowmeter was about 500 kg/hr. The ash flowrate obtained with the flowmeter was slightly higher than what was measured by momentarily diverting the ash flow into a barrel. The discrepancy is believed to be due mainly to inaccuracies in the calculation of the inlet and outlet bulk temperatures of the ash.

The average heat transfer coefficient over the tube bundles within the ash flowmeter were similar in magnitude to those measured using cylindrical electrically heated probes in the downcomer of the cold model circulating fluidized bed at UNB and were in the range of 100 to 200 $W/m^2 \cdot °C$.

The measurements in the downcomer at UNB have shown that only the sides of a horizontal cylinder immersed in a packed bed of solids moving vertically downward are in contact with fast moving solid particles; the top portion of the cylinder is covered with a layer of nearly stagnant particles whereas its underside is exposed to an air gap. The average heat transfer coefficient over the surface of the cylinder decreases with increasing probe size and increases slightly with increasing solids flux and decreasing head of solids above the cylinder.

In both the vertical downcomer at UNB and in the inclined return pipe at CFB Summerside, the solids flow was in a moving packed bed mode. However in the return pipe at CFB Summerside, the solids did not occupy the entire cross-section of the pipe; a 4 cm thick channel apparently created by upward flowing air from the J-valve was present near the upper inside wall of the pipe.

8. RECOMMENDATIONS

The ash flowmeter developed in this study for measuring ash recirculation rates should be used preferably in vertical downcomers to avoid the air channelling problem that can occur with inclined return pipes. When it is used in an inclined downcomer, one should attempt to determine the amount of heat picked up by the upflowing air by measuring the inlet and outlet temperatures and the flowrate of the air.

When installing the ash flowmeter, necessary measures should be taken to ensure that the ash will be of uniform temperature at the inlet of the heat exchanger and that the heat loss to the surroundings will be negligible.

It has been demonstrated in this study that a horizontal cylinder is a poor heat exchange surface in a packed bed of solids moving vertically downward. A more effective geometry might be that of an elliptical tube with its major axis oriented parallel to the solids flow. A larger fraction of the perimeter of this tube should be in contact with fast moving particles and as a result higher heat transfer coefficients and more compact heat exchanger designs should be obtained. The heat transfer coefficient over the elliptical tube might also be a stronger function of solids flux, and this relationship may then be used to determine the ash recirculation rate from the measurement of the average heat transfer coefficient over a single tube. Further work is required to evaluate this design alternative.

9. REFERENCES

1. Couturier, M.F., Doucette, B. and Poolpol, S.: A Study of Gas Concentration, Solids Loading and Temperature Profiles within the Chatham CFB Combustor, final report to Energy, Mines and Resources Canada under contract 23440-8-9153/01-SS (1989).

2. Becker, H.A. and Code, R.K.: The Pilot Installation at Queen's University for Studies of Atmospheric Fluidized Bed Combustion, report QFBC.TR.82.1, Queen's University, Kingston, Ontario (1982).

3. Yerushalmi, J., Turner, D.H. and Squires, A.M.: Ind. Eng. Chem. Proc. Des. Dev., 15, 47-53 (1976).

4. Burkell, J.J., Grace, J.R., Zhao, J. and Lim, C.J.: Measurement of Solids Circulation Rates in Circulating Fluidized Beds in Circulating Fluidized Bed Technology II ed. by Bassu, P. and Large, J.F., 501-509 (1988).

5. Salib, P.: Investigation of Sulphur Capture during Circulating Fluidized Bed Combustion of Eastern Canadian Coals (Phase II), Report no. MDP/88/17, RPC, Fredericton, N.B. (1989).

6. Incropera, F.P. and DeWitt, D.P.: Fundamentals of Heat and Mass Transfer, 2nd ed., John Wiley & Sons (1985).

7. O'Dea, D.P., Rudolph, V., Chong, Y.O. and Leung, L.S.: Powder Technology, 63, 169-178 (1990).

8. Stull, D.R. and Prophet, H., ed.: Janaf Thermochemical Tables (2nd ed.), U.S. Dept. of Commerce, Springfield (1971).

9. Sarana, J.C. and Talbot, J.D.: Prog. Energy Combust. Sci., 1, 73-102 (1984).